# Spatial Relationship between Precipitation and Runoff in Africa

Fidele Karamage[1,2,3,4], Yuanbo Liu[1], Xingwang Fan[1], Meta Francis Justine[2,5], Guiping Wu[1], Yongwei Liu[1], Han Zhou[1], Ruonan Wang[1]

[1]Key Laboratory of Watershed Geographic Sciences, Nanjing Institute of Geography & Limnology, Chinese Academy of Sciences, Nanjing 210008, People's Republic of China
[2]University of Chinese Academy of Sciences, Beijing 100049, People's Republic of China
[3]University of Lay Adventists of Kigali, Kigali, P.O. Box 6392, Rwanda
[4]Joint Research Center for Natural Resources and Environment in East Africa, Kigali, P.O. Box 6392, Rwanda
[5]Chengdu Institute of Biology, Chinese Academy of Sciences, Chengdu 610041, People's Republic of China

*Correspondence to*: Yuanbo Liu (ybliu@niglas.ac.cn, yb218@yahoo.com)

**Abstract.** Apart from the challenges of runoff prediction in ungauged watersheds around different parts of the world, the direct use of river discharges on non-catchment regional studies (i.e.: country scale) also seems to be an unrealistic method that requires scientific precautions. Hence, this study intends to estimate the relationship between precipitation and runoff within 25 major basins and all 55 countries of the African continent. Initially, observed runoff coefficients were estimated from monthly runoff (R) data calculated from historical streamflow records provided by the Global Runoff Data Centre (GRDC) and monthly precipitation (P) datasets from the Global Precipitation Climatology Centre (GPCC) for the period spanning from 1901 to 2016. Subsequently, the observed runoff coefficients for 535 catchments covering about 47.43% of the whole continent were downscaled at 0.5° grid scale based on grids' direct runoff contributions to their corresponding basins estimated following the Natural Resources Conservation Service (NRCS) runoff curve number (CN) approach. NRCS-CN involves the land use and land cover (LULC) information, soil hydrological characteristics, antecedent soil moisture condition (AMC) estimated according to an antecedent precipitation index (API) and precipitation. Predictions in ungauged basins (PUB) were achieved using the inter-gauged and ungauged basin parameter transfer method based on spatial hydrologic similarities. Monthly hydrologic similarity's feature datasets were developed from the key runoff controlling factors, including AMC, CN, terrestrial water storage change (TWSC), surface temperature (T), and topographic parameters (topographic wetness index (TWI) and slope). The results indicated that 14% of the annual mean P (671.88 $mm \cdot yr^{-1}$) became R (94.9 $mm \cdot yr^{-1}$), and the remaining 86% (576.98 $mm \cdot yr^{-1}$) evapotranspirated over the continent. Spatial analysis reveals that the monthly and annual P-R relationship varied significantly among different basins and countries, mainly due to their climatic conditions. Generally, the highest runoff depths and runoff coefficients were observed in humid tropical regions associated with higher precipitation intensities compared to subtropical and temperate drylands.

**Keywords**: Africa; basin; runoff curve number; precipitation; runoff coefficient; water balance.

## 1 Introduction

In the 21st century water resources management becomes a major concern to human life and environmental protection (Cosgrove and Loucks, 2015). It is well-known that precipitation is the source of freshwater on our planet, and its intensity varies from one region to another. Precipitation-to-runoff is the main source of water for rivers, lakes and ocean replenishment (Edwards et al., 2015). Water scarcity aggravates poverty to an estimate of 300 million people living in the drylands of Africa and the number is expected to increase by 65-80% in 2030 (Cervigni and Morris, 2016). By 2050, it is estimated that 40% of the global population will be exposed to river basins that experience severe water stress, particularly in Africa and Asia (UNISDR, 2015). Droughts further induce severe environment degradation, social conflicts and hunger crisis (Messer et al., 2001;Clover, 2003). On the other hand, intensive runoffs cause significant damages such as soil erosion, floods, landslides, water pollution, and infrastructure destructions (Goudie, 2000;Weng, 2001;Karamage et al., 2017a). For instance, the population exposed to floods increased from 0.5 to 1.8 million between 1970 and 2010 in Sub-Saharan Africa (UNISDR, 2011). Water-related problems have far-reaching effects in Africa, where, limited financial funds, sparse hydrological data and reliable scientific information bothers sustainable planning and management of water resources and related disasters (Oyebande, 2001;Karamage et al., 2016;Urroz et al., 2001).

Geographical Information System (GIS) has evolved since its introduction in the 1960s, and now becomes a widely used tool able to deal with multiple variables regarding basin management. However, GIS-based hydrological studies rely strongly on databases (Terakawa, 2003). Various runoff-related studies have been carried out with different purposes such as, for example, runoff depth estimation at global scale (Hong et al., 2007;Fekete et al., 2002a) (Hong et al., 2007;Fekete et al., 2002b;Ruess, 2015;Smakhtin, 2004) and water stress assessment at country and global scales (Ruess, 2015;Smakhtin, 2004), modelling blue and green water availability in Africa (Schuol et al., 2008) and runoff predictions in different parts of Africa (Tesemma et al., 2010;Olang and Fürst, 2011;Jaleta et al., 2017;Mahmoud, 2014;Karamage et al., 2017a). However, based on our knowledge, there is no available detailed study on the relationship between precipitation and runoff in Africa indicating how river discharges available at catchment scale can be downscaled at small unity of land or grid scale which could be utilized reasonably to estimate P-R correlation at a non-catchment spatial scales (i.e.: countries, etc.), taking into consideration well-known key runoff controlling factors such as land use, climate, soil characteristics, etc. Briefly, this study aims at assessing the relationship between precipitation and runoff within 55 African countries and 25 major drainage basins. As scientific contribution, this study highlighted step by step how the Natural Resources Conservation Service (NRCS) runoff curve number (CN) can be a prominent proxy for the basin's river discharge downscaling at a grid scale which can be reasonably utilized on the non-catchment regional studies (i.e.: Country scale). Actually, runoff-related studies are often conducted at a drainage basin scale, but, hydrological studies on the grid and country scales are very useful at national level since each government has own policies for water resource management. For instance, it has been noticed that runoff discharges are useful in water stress analysis on country scale (Ruess, 2015;Smakhtin, 2004). Integration of NRCS-CN in downscaling the runoff discharges do not alter the quantity of observed runoff at a catchment scale, but it redistributes catchment's discharged runoff volume to its

grids proportionally according to their respective climate and physical conditions. NRCS-CN is very useful in various hydrological studies mainly in predicting the direct runoff discharges by incorporating the land use and land cover (LULC) information, soil hydrological characteristics, antecedent soil moisture condition (AMC) and precipitation (Hawkins, 1993). Besides this, the prediction of the P-R relationship in ungauged regions was achieved utilizing the inter-gauged and ungauged basin parameter transfer method that was previously recommended in other hydrological studies as a reliable approach for parameter predictions in ungauged basins (PUB) (Bárdossy, 2007;Blöschl, 2006). Using this method, the gridded observed runoff coefficients ($Or_c$) were transferred to ungauged regions according to their hydrologic similarity. Monthly hydrologic similarity's feature datasets were established from key runoff controlling factors such as: (i) AMC, (ii) NRCS-CN, (iii) terrestrial water storage change (TWSC), (iv) land-surface temperature (T), and (v) topographic parameters (topographic wetness index (TWI) and slope). The present study developed a unique monthly hydrologic similarity feature dataset with multiple zones. Each zone is composed by a set of grids with similar climatic and physical characteristics. The runoff controlling factors were firstly classified into ranges, converted to non-simplified polygons and stacked together using an overlay (intersect) analysis technique (Zhu, 2016) performed with the "intersect tool" available in "overlay tools", one of the "Analysis tools" in ArcMap v.10.5. After that, the mean observed runoff coefficients were transferred to ungauged regions employing the "Zonal Statistics as Table Tool" available in "Zonal tool" of the "Spatial Analyst Tools" in ArcMap v.10.5" where, hydrologic similarity dataset were considered as "Input raster or feature zone data", and gridded observed runoff coefficient as "Input value raster". Inter-gauged and ungauged basin parameter transfer approach was chosen to be used in this study because of its simplicity and reasonable prediction in ungauged regions, yielding the results representing a real-world phenomenon occurring in the same region. This method can be considered as one of the hybrid interpolation or gaps filling techniques which are very useful in developing various datasets such as temperature, precipitation, soil, etc.

## 2 Data inputs and Methods

### 2.1 Study area

Africa (Figure 1) is the world's second-largest continent (≃ 30.3 million km²) accounting for 6% of Earth's surface area and 20.4 % of land area (Sayre and Pulley, 1999;Mawere, 2017). It is the second-most-populous continent (1,256 million people) after Asia (4,504 million people) as of 2017 (UN-DESA, 2017). Statistical computation from the European Space Agency (ESA) Climate Change Initiative (CCI) land cover (LC) map 2015 (ESA-CCI, 2017) showed that Africa is comprised of forests (24.52%), grassland (24.51%), cropland (16.14%), built-up areas (0.16%), wetlands (0.84%), inland water (0.99%), and bare areas (32.84%).

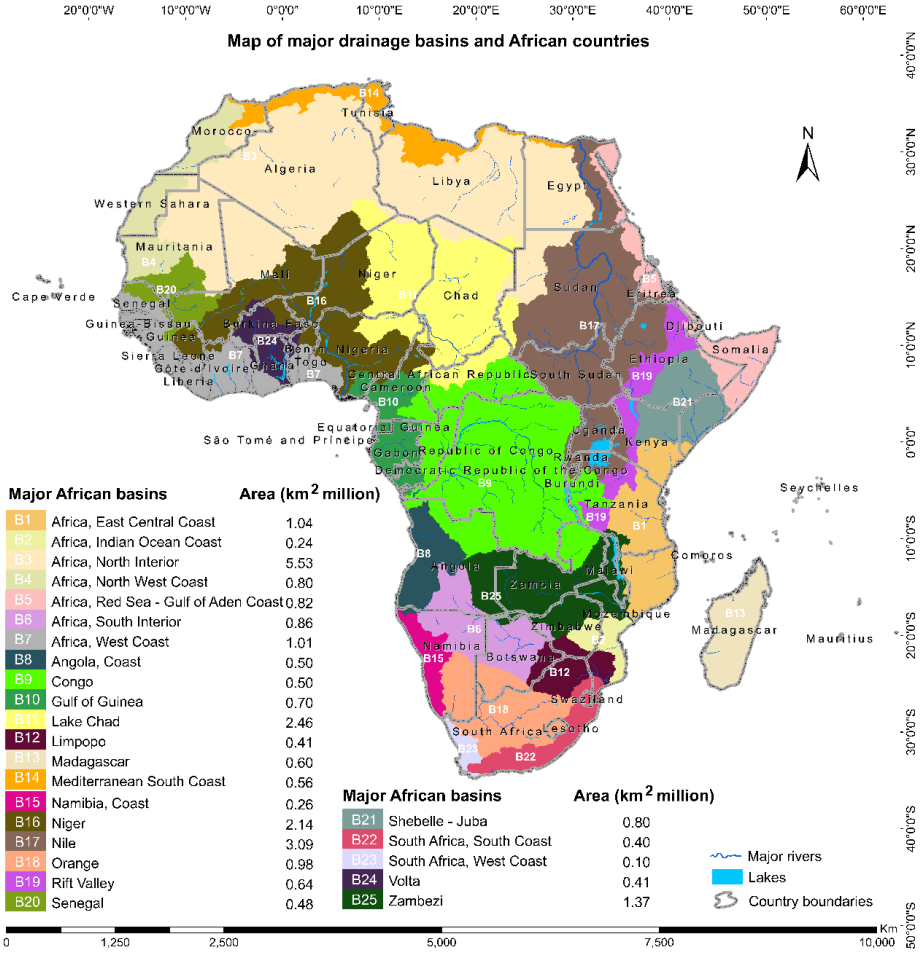


**Figure 1.** Hydrological map showing major rivers, lakes, 25 major basins (FAO, 2009) and 55 countries of Africa (GADM, 2015).

Over 60% of the soil is dominated by hot, arid or immature soil assemblages: Arenosols (22%), Leptosols (18%), Cambisols (11%), Calcisols (5%), Regosols (3%) and Solonchacks/Solonetz (2%). Another 20% is characterized by tropical or sub-tropical features: Ferralsols (10%), Plinthisols (5%), Lixisols (4%) and Nitisols (2%) (Dewitte et al., 2013). Based on the Climatic Research Unit Timeseries (CRU TS) land-surface temperature datasets (1901 – 2016) (Harris et al., 2014), and the GPCC datasets (1901 – 2016) (Markus et al., 2018), the African continent has an overall long-term mean surface temperature (T) of 24°C·yr$^{-1}$ and mean precipitation (P) of 671.88 mm·yr$^{-1}$. Africa has three major climate types including tropical (T = 25°C·yr$^{-1}$; P = 836.36 mm·yr$^{-1}$), subtropical (T = 22°C·yr$^{-1}$; P = 146.23 mm·yr$^{-1}$) and temperate zones (T = 18°C·yr$^{-1}$; P = 257.34 mm·yr$^{-1}$). The topography is characterized by large-scale extensional features such as the East African Rift, anomalously subsided basins and uplifted domes (Moucha and Forte, 2011). The continent is divided into 25 major hydrological basins according to its hydrological characteristics (FAO, 2009). Approximately, 60% of the African continent

is drained by 10 large rivers (Congo, Limpopo, Niger, Nile, Ogooue, Orange, Senegal, Shebelle, Volta and Zambezi) and their tributaries (Paul et al., 2014).

### 2.2 Datasets and Application

The data were processed and analysed using the Esri ArcGIS software version 10.5, SDMToolbox version 2.2 (Brown et al., 2017) and Excel VBA (Visual Basic for Applications) (Walkenbach, 2010). Figure 2 demonstrates the conceptual framework used to analyze the relationship between precipitation and runoff in Africa.

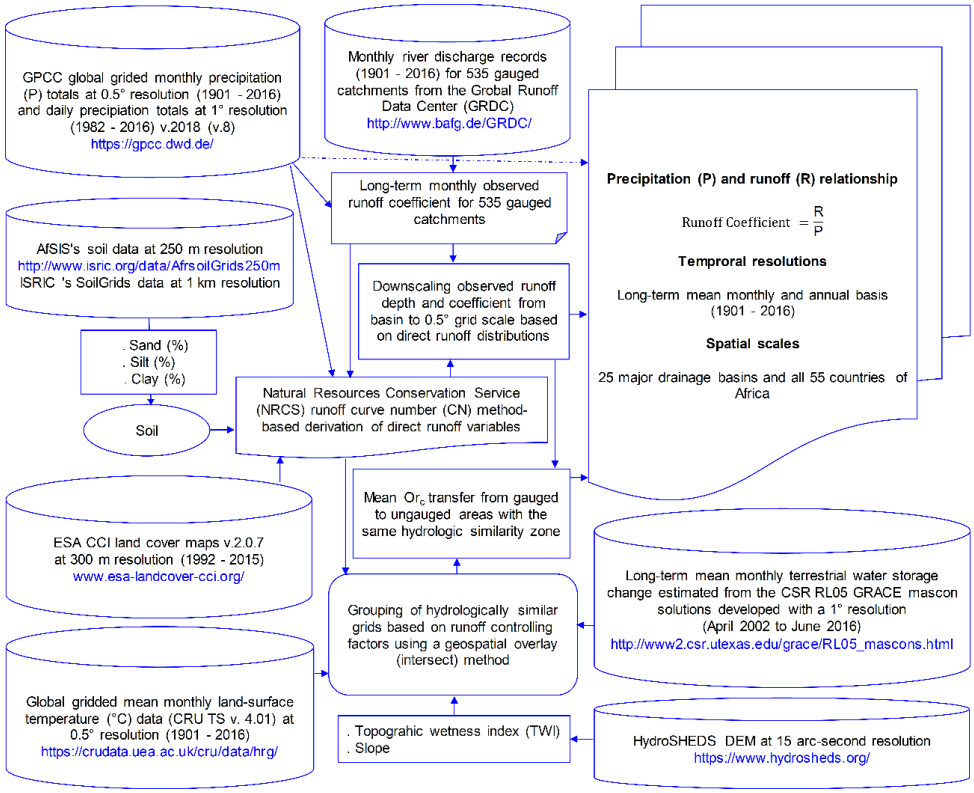


**Figure 2.** A conceptual framework used for analyzing the precipitation-runoff relationship in Africa.

#### 2.2.1 Runoff estimation in gauged catchments

The runoff coefficients over gauged catchments were estimated with two types of data: (1) the monthly time series of river discharge data for 535 African catchments (Figure 3) discontinuously recorded since 1901 until 2016 were provided by request from the Global Runoff Data Centre (GRDC). The GRDC is an international organization based in Germany, a branch of the World Meteorological Organization (WMO) that was established in 1988 to support scientific studies on global climate change and water resources management (GRDC, 2018), and (2) monthly precipitation datasets acquired from the Global Precipitation Climatology Centre (GPCC) Full Data Gridded Monthly Totals Version 2018 (V.8) at 0.5° resolution for the period 1901–

2016. GPCC product is a Rain-Gauges built on GTS-based and Historical Data that is operated by the German Weather Service (DWD) under the auspices of the World Meteorological Organization (WMO) (Markus et al., 2018).

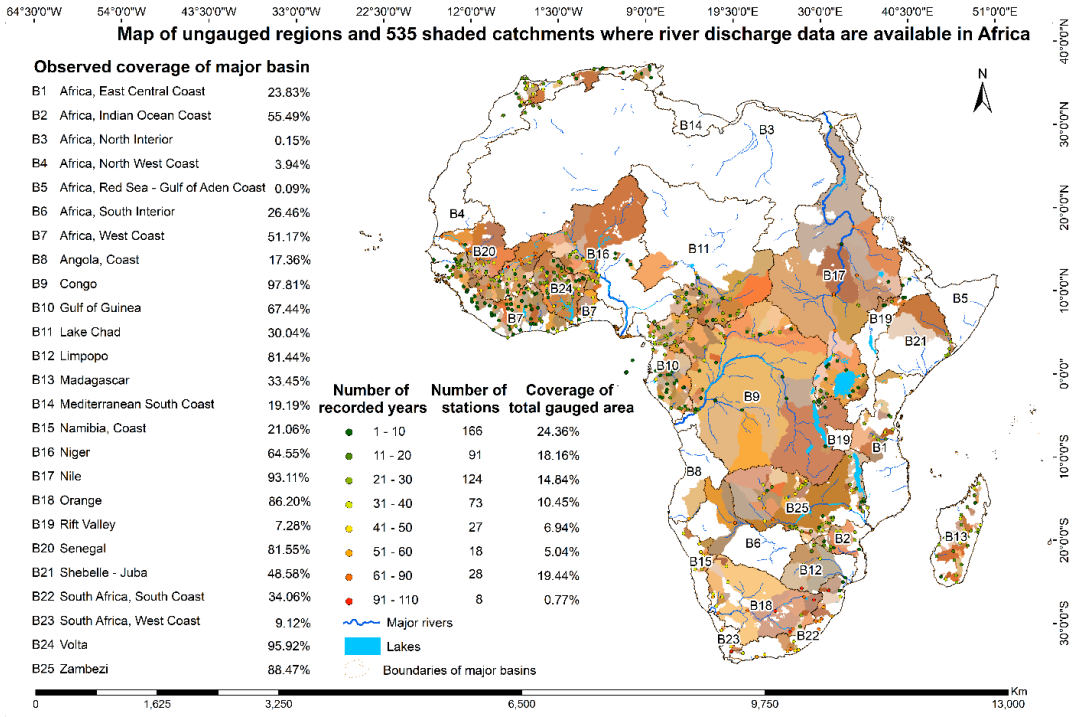


**Figure 3.** Distribution of 535 GRDC gauged catchments (covering ≃ 47.43% of the total African continent) and streamflow gauging stations (GRDC, 2018) within 25 major basins of Africa (FAO, 2009).

On account of discharge data that were discontinuously recorded which could not allow the possibility of monthly or annual accurate trend analysis, the final results of the present study were generated at the long-term monthly and annual mean temporal resolution. By following Eq. (1) (Kadioglu and ŞEN, 2001), a runoff coefficient is estimated as the ratio of mean runoff depth to rainfall intensity for each catchment. The monthly runoff coefficients were estimated for each month whenever runoff discharge was recorred. Then, all historical monthly coefficients were summed and divided by the number of recorded months to obtain the long-term monthly average runoff coefficient for each station.

The annual runoff depth (mm·yr-1) is the total of monthly runoff depths for all 12 months of a year. The average annual runoff coefficient is estimated as the ratio of annual runoff depth (mm·yr$^{-1}$) to the annual precipitation intensity (mm·yr$^{-1}$).

$$Orc_b = \frac{Or_b}{P} \quad (1)$$

where, $Orc_b$ is the basin's observed average monthly runoff coefficient (dimensionless), $Or_b$ is the basin's observed runoff depth (mm·month$^{-1}$) and $P$ is precipitation intensity (mm·month$^{-1}$).

The runoff coefficient is usually a suitable proxy to assess the correlation between precipitation and runoff due to its absolute capability to indicate the ratio of runoff (R) generated by the total precipitation (P) amount within a catchment (Kadioglu and ŞEN, 2001), it has values varying from 0 (low P-R correlation) to 1 (high P-R correlation) (Blume et al., 2007). In addition, runoff coefficient is very useful for rainfall runoff management in different land cover types since it can easily identify the ratio of rainwater flowed from each land use type under heterogeneous climate and physical conditions among different grids of the catchment. It may help to locate areas with high potential runoff risk which require special practices of stormwater management (Chen et al., 2007). Higher runoff coefficient values are often observed on impervious surfaces and unwell-managed croplands due to their low infiltration capacity compared to other land use classes such for example grasslands and forests (Goudie, 2000; Weng, 2001). Areas with low runoff coefficients are those with a relatively higher infiltration and/or evapotranspiration ($E_T$) rates. Underground water storage change also plays significant role in runoff generation process throughout the alteration of soil moisture condition. However, in the long-term annual mean basis of water balance analysis, the estimation of terrestrial water storage change provides approximately zero values due to a variety of wet and dry seasons (Long et al., 2014).

### 2.2.2 Runoff estimation in ungauged catchments

Runoff coefficients over ungauged regions were estimated using the inter-gauged and ungauged parameter transfer method based on the hydrologic similarity feature zones established by means of overlay (intersect) technique applied to major runoff controlling factors, including AMC, CN, TWSC, T, TWI and slope that were selected among others based on their potential effect in runoff generation process as previously revealed by different researchers (Liu and De Smedt, 2004;Bárdossy, 2007;Yuting et al., 2011;McCabe and Wolock, 2011). Inter-gauged and ungauged parameter transfer method is one of acceptable approach for parameter predictions in ungauged Basins (PUB) recommended in different hydrological studies (Bárdossy, 2007;Blöschl, 2006;Chiew et al., 2018). Several hydrologic models are available and utilized in different projects; but, most of them limited either due to their different input parameter requirements, a lot of time required for preparing input data, and complexity model setting (Lim et al., 2006). Ungauged regions accounting 52.57% of the total continent of Africa seems to be larger extent compared to the recorded catchments (47.43% of African continent) (Figure 3) due to 31% of the continent occupied by the desert of Sahara (Cook and Vizy, 2015) where the runoff depths and runoff coefficient is approximately 0 due to absence of precipitation in this region. The remaining ungauged regions account only 21.57% of the total African continent and are distributed in different climatic zones where it is possible to predict their hydrologic conditions based on the observed parameters of neighbouring gauged catchments. Using any other model for P-R correlation assessment it might be a double task since it would be necessary to calibrate the results using almost the same method of hydrologic similarity analysis.

### 2.2.2.1 Estimation of direct runoff using the NRCS-CN method

NRCS-CN is one of the ancient popular and efficient empirical hydrologic approaches adopted by various researchers worldwide for water resources planning and assessment, especially estimating the direct rainfall-runoff. It was developed in 1956 by the United States Department of Agriculture (USDA) Natural Resources Conservation Service (NRCS) (Cronshey, 1986;Silveira et al., 2000). This method is easily understandable, simple and useful for direct runoff prediction over ungauged catchments (Mishra et al., 2006). CN is generally considered as a major input parameter in many hydrologic models such as for example the Long-Term Hydrologic Impact Assessment (L-THIA) model (Lim et al., 2006), the Hydrologic Modelling System (HEC-HMS) (Engineers, 2008;Halwatura and Najim, 2013), The Chemicals, Runoff, and Erosion from Agricultural Management Systems (CREAMS) (Knisel and Douglas-Mankin, 2012), Simulation of Production and Utilization of Rangelands (SPUR) model (Wright and Skiles, 1987). NRCS-CN method predicts the $Dr_c$ and Dr by involving the land use and land cover (LULC) data, soil hydrological characteristics and antecedent soil moisture condition, according to an antecedent precipitation index (API) and precipitation (Cronshey, 1986). The LULC maps (Figure 4) used in this study were reclassified from time series of annual global Climate Change Initiative Land Cover (CCI-LC) maps at 300 m spatial resolution covering a period of 24 years (1992 – 2015) (ESA-CCI, 2017).

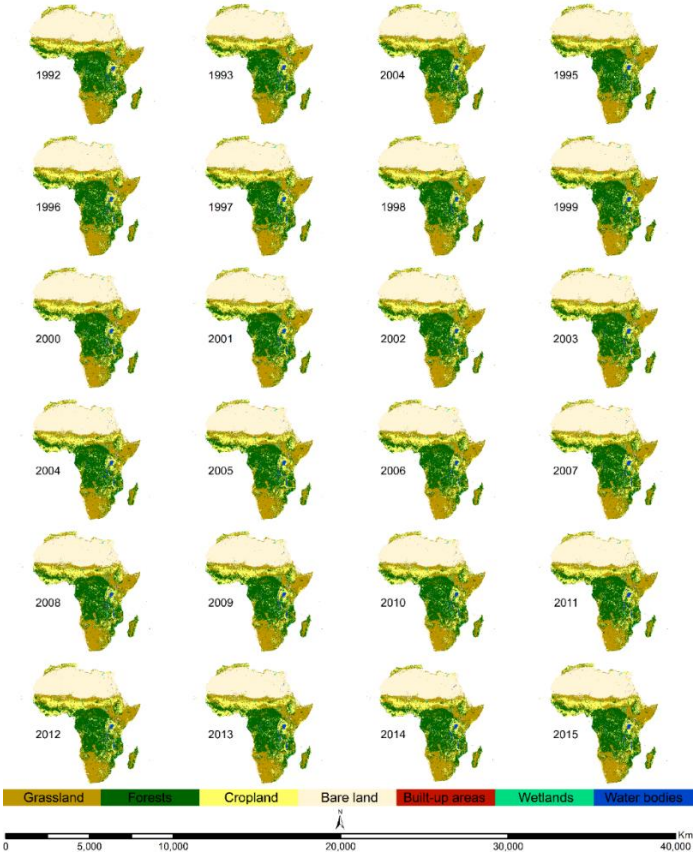


**Figure 4**. A time series of annual land cover maps (ESA-CCI, 2017) of Africa with reclassified 7 classes (1992 – 2015).

These land cover maps were originally classified from the landcover imagery captured by five different satellites, including the Advanced Very High-Resolution Radiometer (AVHRR), Medium Resolution Imaging Spectrometer Full Resolution and Reduced Resolution (MERIS FR and RR), SPOT-Vegetation (SPOT-VGT), Project for On-Board Autonomy, with the V standing for Vegetation (PROBA-V), Environmental Satellite-Advanced Synthetic Aperture Radar (ENVISAT-ASAR). The CCI-LC map 2015 was validated using the GlobCover map 2009 with two overall accuracy levels of 71.45% and 75.4% (ESA-CCI, 2017). Based on the CCI-LC product manual version 2.0 (ESA-CCI, 2017), we have reclassified all 24 CCI-LC maps from the LCCS (Land Cover Classification System) legend to IPCC (Intergovernmental Panel on Climate Change) legend (Penman et al., 2003) that are more compatible with the NRCS-CN structure.

The recent updated dataset of sand, clay, and silt fractions available at ≃ 250 m resolution were downloaded from the Africa Soil Information Service (AfSIS) database (Hengl et al., 2015) and used to classify the soil texture dataset of Africa (Figure 5). Soil texture data were utilized in conjunction with LULC maps (Figure 4) for the development of hydrologic soil group (HSG) and CN dataset (Figure 5) following the studies of Yeo et al. (2004) , Cronshey (1986), and Sumarauw and Ohgushi (2012) (Table 2). Because the AfSIS data have gaps over the Sahara desert, in this region the soil texture was classified from the WorldGrids' s sand, clay, and silt fractions available at ≃ 1 km spatial resolution (Hengl et al., 2014). Soil texture was classified referring to table 1 adapted from the soil textural triangle developed by the United States Department of Agriculture (USDA) (Fernandez-Illescas et al., 2001).

**Table 1**. Soil texture classes adapted from the USDA' s soil textural triangle (Fernandez-Illescas et al., 2001).

| Soil Texture Name | Sand (%) | Silt (%) | Clay (%) |
|---|---|---|---|
| Sand (Sa) | 85 – 100 | 0 – 15 | 0 – 10 |
| Loamy sand (LoSa) | 70 – 90 | 0 – 30 | 0 –15 |
| Sandy loam (SaLo) | 43 – 80 | 0 – 50 | 0 – 20 |
| Loam (Lo) | 23 – 52 | 28 – 50 | 7 – 27 |
| Silty loam (SiLo) | 0 – 50 | 50 – 88 | 0 – 27 |
| Silt (Si) | 0 – 20 | 88 – 100 | 0 –12 |
| Sandy clay loam (SaClLo) | 45 – 80 | 0 – 28 | 20 – 35 |
| Clay loam (ClLo) | 20 – 45 | 15 – 53 | 27 – 40 |
| Silty clay loam (SiClLo) | 0 – 20 | 40 – 73 | 27 – 40 |
| Sandy clay (SaCl) | 45 – 65 | 0 – 20 | 35 – 45 |
| Silty clay (SiCl) | 0 – 20 | 40 – 60 | 40 – 60 |
| Clay (Cl) | 0 – 45 | 0 – 40 | 40 – 100 |

**Table 2**. LULC classes and their corresponding HSG, soil texture and CN (adapted from (Yeo et al., 2004;Cronshey, 1986;Sumarauw and Ohgushi, 2012).

| LULC | Soil Texture | HSG | CN |
|---|---|---|---|
| Grass | Sand, loamy sand, or sandy loam | A | 35 |
| | Silt loam or loam | B | 56 |
| | Sandy clay loam | C | 70 |
| | Clay loam, silty clay loam, sandy clay, silty clay, or clay | D | 77 |
| Forrest | Sand, loamy sand, or sandy loam | A | 30 |
| | Silt loam or loam | B | 55 |
| | Sandy clay loam | C | 70 |
| | Clay loam, silty clay loam, sandy clay, silty clay, or clay | D | 77 |
| Agriculture | Sand, loamy sand, or sandy loam | A | 64 |
| | Silt loam or loam | B | 75 |
| | Sandy clay loam | C | 82 |
| | Clay loam, silty clay loam, sandy clay, silty clay, or clay | D | 85 |
| Barren | Sand, loamy sand, or sandy loam | A | 77 |
| | Silt loam or loam | B | 86 |
| | Sandy clay loam | C | 91 |
| | Clay loam, silty clay loam, sandy clay, silty clay, or clay | D | 94 |
| Urban | Sand, loamy sand, or sandy loam | A | 81 |
| | Silt loam or loam | B | 88 |
| | Sandy clay loam | C | 91 |
| | Clay loam, silty clay loam, sandy clay, silty clay, or clay | D | 93 |
| Wetland | Sand, loamy sand, or sandy loam | A | 0 |
| | Silt loam or loam | B | 62 |
| | Sandy clay loam | C | 74 |
| | Clay loam, silty clay loam, sandy clay, silty clay, or clay | D | 85 |
| Water | Sand, loamy sand, or sandy loam | A | 100 |
| | Silt loam or loam | B | 100 |
| | Sandy clay loam | C | 100 |
| | Clay loam, silty clay loam, sandy clay, silty clay, or clay | D | 100 |

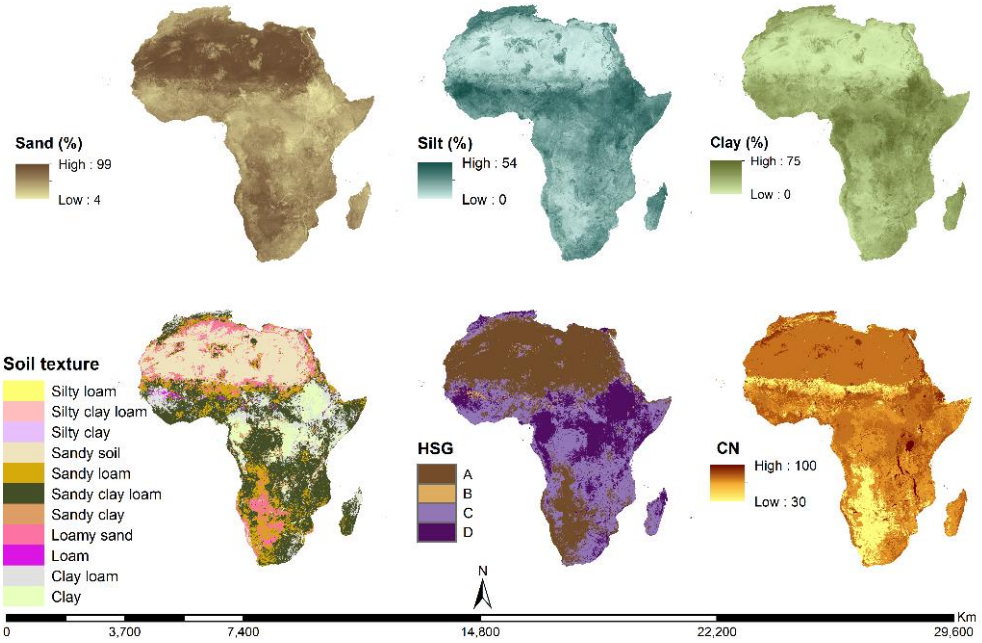


**Figure 5**. Maps of sand, clay, and silt fractions, soil texture, hydrological soil group (HSG) and long-term mean curve number (CN) unadjusted by AMC (1992 – 2015).

Adjusted long-term monthly CN maps (Figure 6) were obtained employing antecedent soil moisture condition (AMC) (Figure 6) using equations (2) and (3) (Hong et al., 2007;Zeng et al., 2017).

$$CN_i^I = \frac{CN_i^{II}}{2.281 - 0.01281 * CN_i^{II}} \quad (2)$$

$$CN_i^{III} = \frac{CN_i^{II}}{0.427 - 0.00573 * CN_i^{II}} \quad (3)$$

$C^I$, $CN^{II}$, and $C^{III}$ are corresponding to AMC I (dry), AMC II (normal), and AMC III (wet), respectively, determined utilizing total 5-day antecedent precipitation index (API) and season types (dormant or passive and active or growing seasons) (Table 3) (Silveira et al., 2000;Hong et al., 2007). The glowing season is considered as the active (wet) season with the precipitation intensity > 100 mm·month$^{-1}$, whilst, the passive (dry) season has a precipitation intensity < 100 mm·month$^{-1}$ (Murray-Tortarolo et al., 2017).

**Table 3**. Seasonal rainfall limits for AMC (Silveira et al., 2000;Hong et al., 2007;Mishra and Singh, 2006).

| AMC group | Total 5-day API (mm) | |
|---|---|---|
| | Dormant (passive) season | Growing (active) season |
| I | < 13 | < 36 |
| II | 13 – 28 | 36 – 53 |
| III | > 28 | > 53 |

Five-day API was estimated using the GPCC Full Data Daily Product V.2018 of daily global land-surface precipitation totals. This product is available at a regular latitude/longitude grid with a spatial resolution of 1° and covers the time period from January 1982 to December 2016 (Anja et al., 2018). The API was estimated following Eq. (4) (Kohler and Linsley, 1951;Heggen, 2001).

$$\text{API} = \sum_{t=1}^{-i} P_t * k^{-t} \quad (4)$$

where, $i$ is the number of antecedent days, $P_t$ is the precipitation amount during day t, and k is a decay constant. It has been revealed that k factor is not critical, its values range from 0.85 to 0.90 over most of the eastern and central portions of the United States where it was well tested (Kohler and Linsley, 1951), and this study used a value of 0.90 that is recommended for the basins without a measured k decay constant (Abdi et al., 2017;Viessman Jr and Knapp, 1977;Heggen, 2001). The NRCS-CN method was modified by different researchers depending on the climatic condition of their study area. The most frequently modified parameter was the initial abstraction coefficient (λ), arguing that the assumption of the λ = 0.2 in the original SCS-CN method seems to be high and suggested that λ with values between 0.01 and 0.05 are more realistic and recommended a value of λ = 0.05 (5% of the storage is assumed as the initial abstraction instead of 20%) because it involves either both lower CN values and small rainfall amount (Yuan et al., 2014;Beck et al., 2009;Shi et al., 2009;Hawkins, 1993;Ponce and Hawkins, 1996;Woodward et al., 2003;Lim et al., 2006). Based on these recent studies, our study used an adjusted SCS-CN equation with a value of λ = 0.05 as demonstrated by Hawkins (1993) with the equations (5), (6) and (7).

$$Dr = \begin{cases} 0 & \text{for } P \leq 0.05 * S \\ \frac{(P - 0.05 * S_{0.05})^2}{P + 0.95 * S_{0.05}} & \text{for } P > 0.05 * S \end{cases} \quad (5)$$

$$S_{0.05} = 1.33 * {S_{0.20}}^{1.15} \quad (6)$$

$$S_{0.20} = \frac{2400}{CN} - 254 \quad (7)$$

where, $Dr$ = the direct runoff (mm), P = rainfall (mm) (Figure 6), $S$ is the maximum potential soil water retention (mm), and $CN$ is the curve number (dimensionless). $I_a = 0.05 * S$ is the initial abstraction (all losses before runoff begins). $Dr_c$ = the direct runoff coefficient (dimensionless) (Figure 6). S is related to the soil and land cover conditions of the watershed through the $CN$ which has a range of 0 to 100 values.

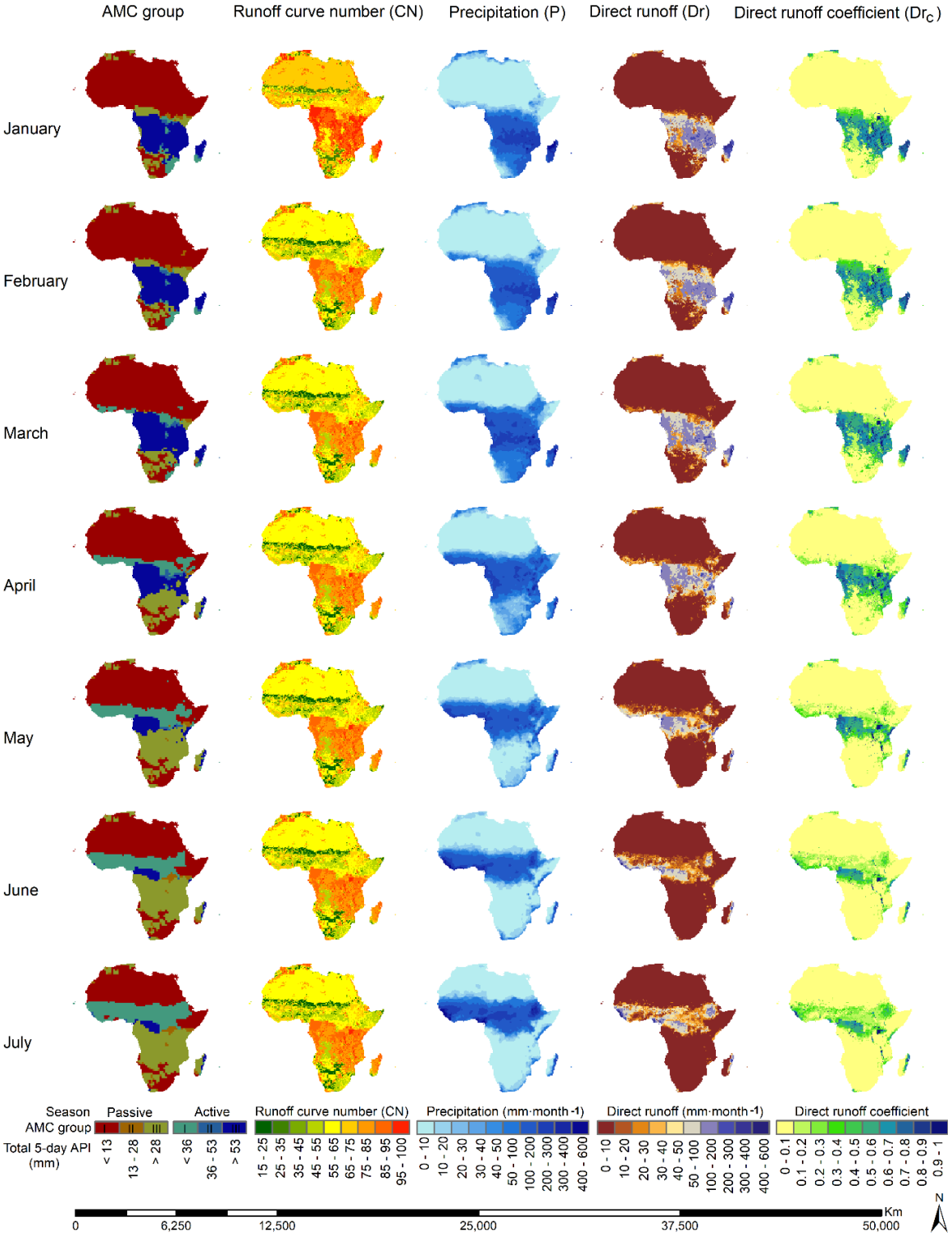
AMC group
Runoff curve number (CN)
Precipitation (P)
Direct runoff (Dr)
Direct runoff coefficient (Drc)
January
February
March
April
May
June
July
Season
Passive
Active
AMC group
Total 5-day API (mm)
< 13
13 - 28
> 28
< 36
36 - 53
> 53
Runoff curve number (CN)
15 - 25
25 - 35
35 - 45
45 - 55
55 - 65
65 - 75
75 - 85
85 - 95
95 - 100
Precipitation (mm·month-1)
0 - 10
10 - 20
20 - 30
30 - 40
40 - 50
50 - 100
100 - 200
200 - 300
300 - 400
400 - 600
Direct runoff (mm·month-1)
0 - 10
10 - 20
20 - 30
30 - 40
40 - 50
50 - 100
100 - 200
200 - 300
300 - 400
400 - 600
Direct runoff coefficient
0 - 0.1
0.1 - 0.2
0.2 - 0.3
0.3 - 0.4
0.4 - 0.5
0.5 - 0.6
0.6 - 0.7
0.7 - 0.8
0.8 - 0.9
0.9 - 1
0
6,250
12,500
25,000
37,500
50,000
Km
N

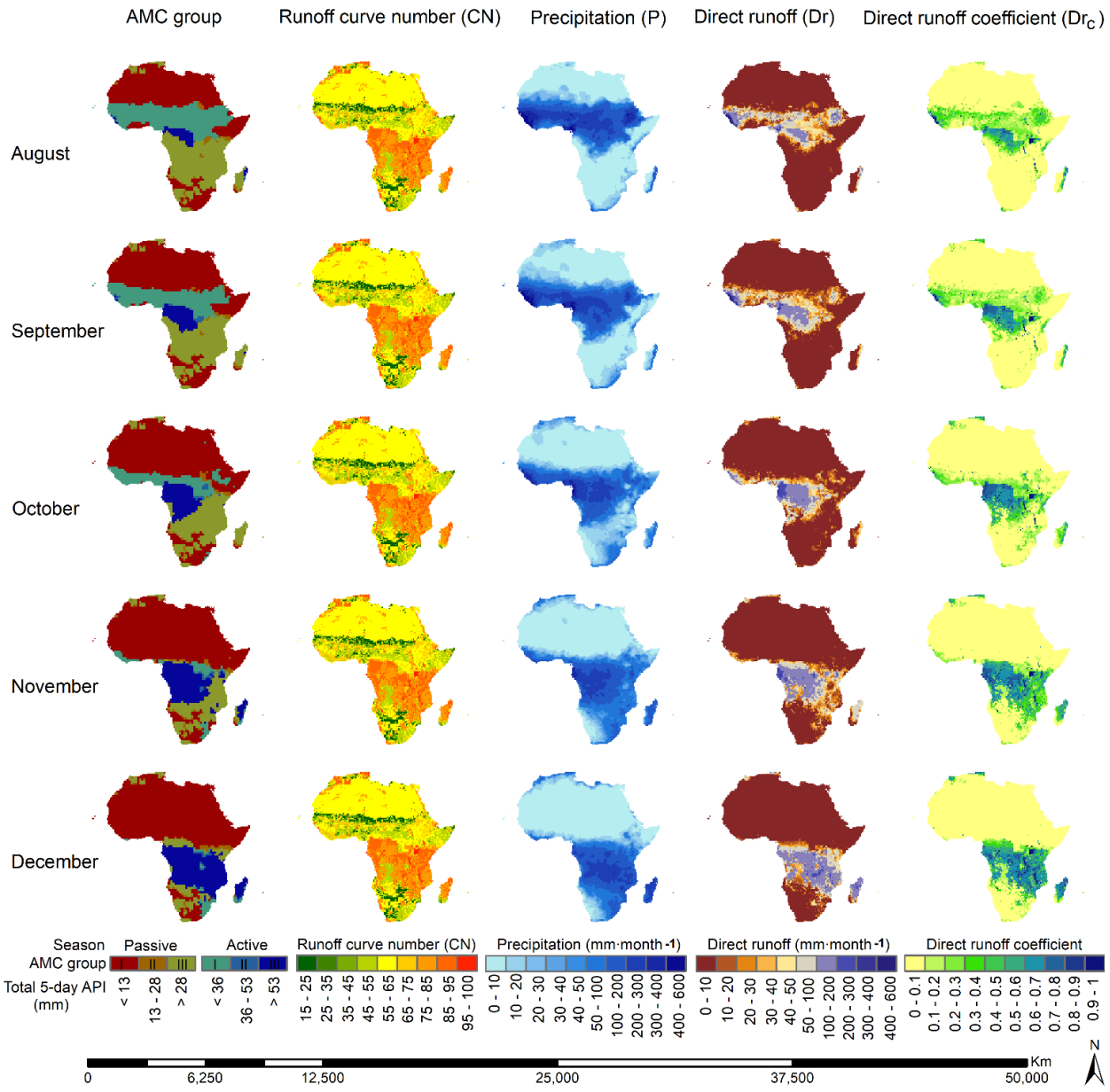


**Figure 6.** Maps of the runoff curve number (CN) adjusted according to antecedent soil moisture condition (AMC), precipitation (P), direct runoff depths (Dr) and direct runoff coefficients ($Dr_c$).

### 2.2.2.2 Downscaling process of the runoff discharges

Equations (8), (9), (10), (11), (12), (13), and (14) express the process used to downscale the observed runoff coefficients and runoff depths from basin scaled to 0.5° grid spatial resolution (Figure 7) based on the direct runoff distributions within different grids of each gauged catchment. This approach provides google results since the mean of observed gridded runoff coefficients and runoff depths equals to the catchment's average observed runoff coefficients and runoff depths, respectively.

$$Drv_g = 0.001 * Dr_g * G \quad (8)$$

$$Drv_b = 0.001 * Dr_b * A \quad (9)$$

$$\emptyset = \frac{Drv_g * 100}{Drv_b} \quad (10)$$

$$Orv_b = 0.001 * Or_b * A \quad (11)$$

$$Orv_g = \frac{Orv_b * \emptyset}{100} \quad (12)$$

$$Or_g = \frac{Orv_g}{G} * 1000 \quad (13)$$

$$Orc_g = \frac{Or_g}{P_g} \quad (14)$$

where, ($\emptyset$) is the percent contribution of each grid's direct runoff volume ($Drv_g$) in $m^3 \cdot month^{-1}$ to its corresponding basin's direct runoff discharge ($Drv_b$) in $m^3 \cdot month^{-1}$, $Dr_g$ is the grid's direct runoff depth ($mm \cdot month^{-1}$), $Dr_b$ is the basin's average direct runoff depth ($mm \cdot month^{-1}$), $G$ is the size of a grid in $m^2$, 0.001 and 1000 are the numbers for unities conversion, $A$ is the drainage area of basin in $m^2$. $Orv_b$ is the basin' s observed runoff discharge ($m^3 \cdot month^{-1}$), $Or_b$ is the basin's observed runoff depth ($mm \cdot month^{-1}$), $Or_g$ is the grid's observed runoff depth ($mm \cdot month^{-1}$), $Orc_g$ is the grid's observed runoff coefficient (dimensionless), $P_g$ is the grid's precipitation intensity ($mm \cdot month^{-1}$).

**2.2.2.3 Application of inter-gauged and ungauged basin parameter transfer approach**

Overlay (intersect) is one of useful geospatial overlay methods that stacks several different types of dataset with the same georeferencing system on top of each other in order to assess the relationship between features of each location. Overlay method has been used in different applications such as relationship analysis between rainfall distribution and elevation, examination of environmental sensitivity based on slope, surface drainage, soil erosion and other environmental parameters (Zhu, 2016). This method was applied to the present study in order to establish a unique zonal feature dataset that combines together a set of important physical-climate variables which control the runoff (AMC, CN, TWSC, T, and TWI and slope). Each intersection of these variables falls within gauged and ungauged grids at the same time, here immediately ungauged grids receive an average of observed runoff coefficient locating within the same intersection. This operation was achieved using the "Zonal Statistics as Table Tool" available in the Spatial Analyst *Tools* of the ArcMap v.10.5" where, hydrologic similarity's zonal feature dataset were considered as "Input raster or feature zone data", and downscaled observed runoff as "Input value raster".

The hydrological similarity analysis involved AMC (Figure 6) based on its potential capability to separate the drying and wetting areas, whilst CN (Figure 6) helps to recognize the effect of land use and soil characteristics in runoff generation process. According to the water balance budget, during the rainy seasons water soaks into pervious ground and once filled in

soil porosities starts to flow into rivers and lakes resulting in an increased level of underground water (acquirers) and surface water reservoirs (rivers, lakes and oceans); in impervious surface rainwater flow forward immediately into surface water reservoirs. Accumulation of water infiltrations improves soil moisture condition and boosts the rate of runoff depths while, a declining water storage phenomenon leads to lower amount of runoff discharge (Edwards et al., 2015). Apart from the natural cause of water storage change fluctuations (i.e.: rainfall and evapotranspiration), human activities (i.e.: water storage for hydropower generation and its release, irrigation, water consumption, etc.) also affect the change of water storage and as well river discharge volume. However, the change of water storage is generally controlled by climate and seasons patterns more than human factors (Edwards et al., 2015).

In order to incorporate the effect of water storage change in hydrologic similarity analysis, this study used the long-term monthly terrestrial water storage change (Figure 7) computed from the Center for Space Research (CSR) Gravity Recovery and Climate Experiment (GRACE) RL05 mascon solutions available at 1$^{o}$ resolution for the period starting from April 2002 to June 2016. The Gravity Recovery and Climate Experiment (GRACE) mission was launched in March 2002 under the NASA Earth System Science Pathfinder (ESSP) Program. GRACE is jointly implemented by the US National Aeronautics and Space Administration (NASA) and German Aerospace Center (DLR) (Save et al., 2016).

The land-surface temperature also plays a big role in water balance where, hot regions are often characterized by higher evapotranspiration rates compared to cold or temperate regions. The long-term monthly land-surface temperature (Figure 7) used in this study was calculated from the 4.01 release of the CRU TS (Climatic Research Unit Timeseries) dataset spanning a period of 116 years (1901 – 2016) (Harris et al., 2014). This dataset was developed, subsequently updated, improved and maintained with support from a number of funders, principally by the UK's Natural Environment Research Council (NERC) and the US Department of Energy. Long-term support is currently provided by the UK National Centre for Atmospheric Science (NCAS), a NERC collaborative center (Harris et al., 2014).

The topography also acts on water flow movement and infiltration; where higher runoff depths are mostly found in regions with steep slopes more than areas with flat and gentle slopes (Ogden et al., 2011). Sometimes, digital elevation model (DEM) is used directly as a parameter that represents the impact of the surface shapes and feature on the hydrological process (Xiao et al., 2017). The dataset of topographic wetness index (TWI) that is also called the Compound Topographic Index (CTI) was developed by Beven and Kirkby (1979) within the runoff model TOPMODEL due to the effect of topography on soil moisture (BEVEN and Kirkby, 1979). TWI (Eq. 15, 16 and 17) that combines local upslope contributing area and slope is commonly used to quantify topographic control on hydrological processes. Higher TWI values represent drainage depressions which are often wet and associated with greater runoff depths compared to crests and ridges relatively with the lower TWI values and dry surfaces that suck a lot of water amount before the beginning of water flow process (Liu et al., 2015;Sörensen et al., 2006;Xiao et al., 2017). TWI and slope parameters (Figure 7) derived from the HydroSHEDS datasets at 15 arc-second resolution (Lehner et al., 2008) were incorporated in the hydrologic similarity analysis of this study in order to separate areas with different topographic features.

$$TWI = \ln\left(\frac{\alpha}{tan\ \beta}\right) \quad (15)$$

$$\alpha = (f + 1) * G \quad (16)$$

$$\beta = (m * (\pi/2)/90 \quad (17)$$

where, α is the upslope area draining through a certain point per unit contour length and β is the slope in radians, $f$ is the flow accumulation calculated from the flow direction that is generated in DEM (meter unity), $G$ is the cell size in $m^2$, $m$ is the slope in degrees, π is pi equals to 3.141592.

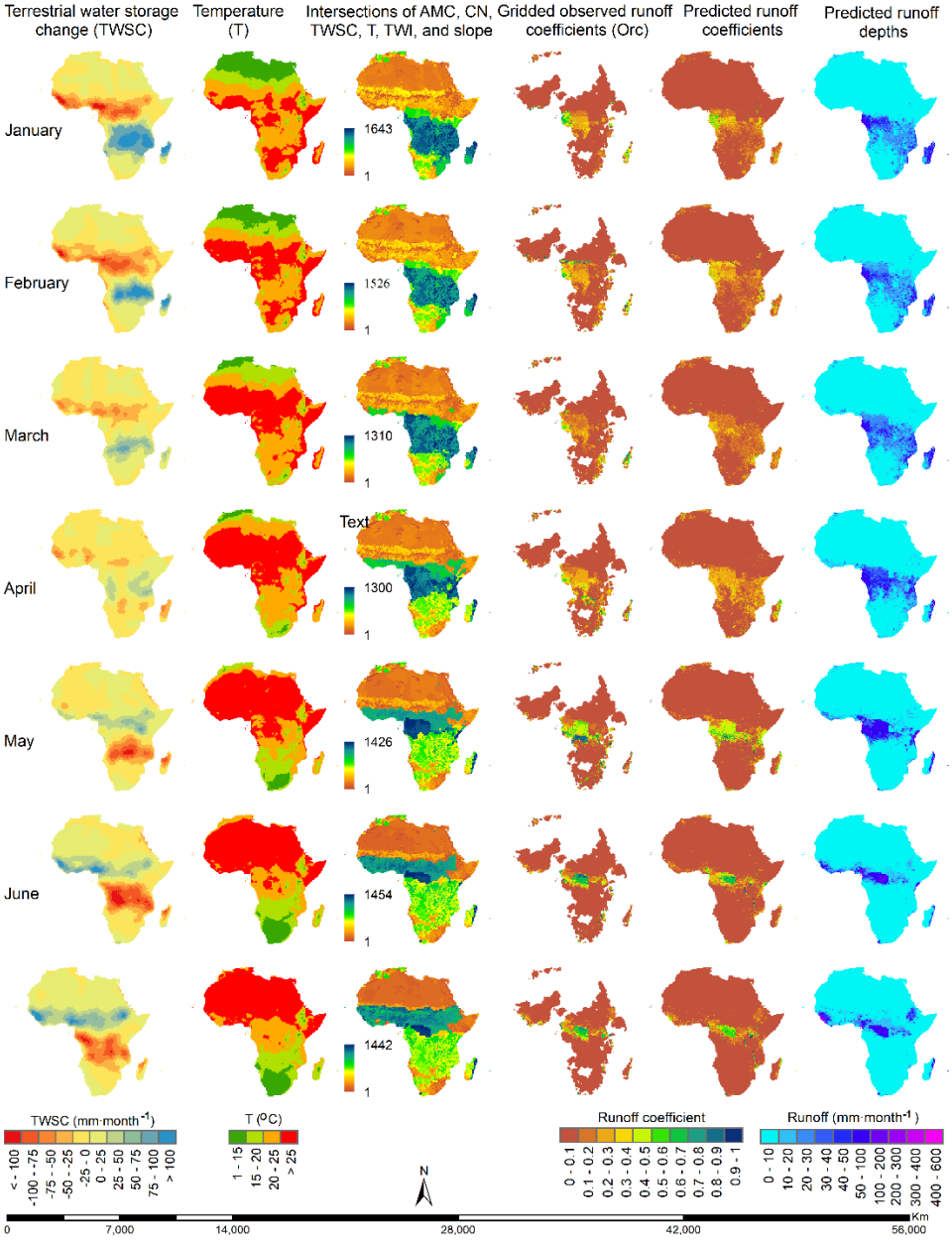

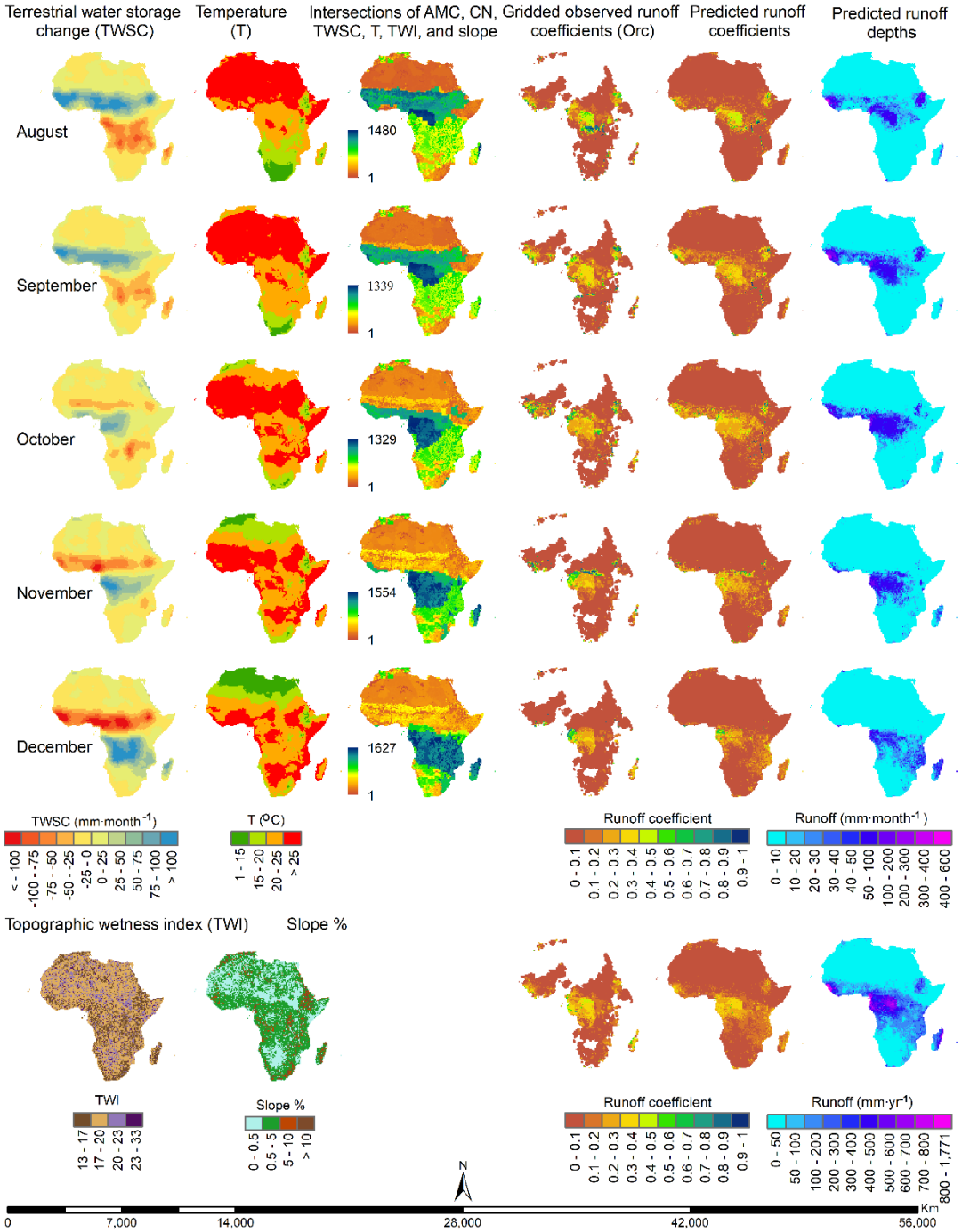


**Figure 7**. Estimated runoff coefficients and runoff depths based on gridded observed runoff coefficients transferred using inter-gauged and ungauged parameter transfer approach, according to hydrological similarity feature dataset resulted from an overlay (intersect) of the runoff controlling factors (AMC, CN (Figure 6), TWSC, T, TWI, and slope).

## 3 Results

Figure 8 presents the final resultant maps obtained by means of the methods above-described in sections 2.2.1 and 2.2.2. Gridded long-term monthly and annual mean runoff coefficients (RC), precipitation (P), and runoff depths (R) were developed at 0.5° spatial resolution (1901 to 2016) and utilized to generate zonal statistics at the continental level (Figure 9 and 10), within 25 major basins (Figure 11), 55 countries of Africa (Figure 12) and as well latitudinal profile (Figure 14 and Table 4).

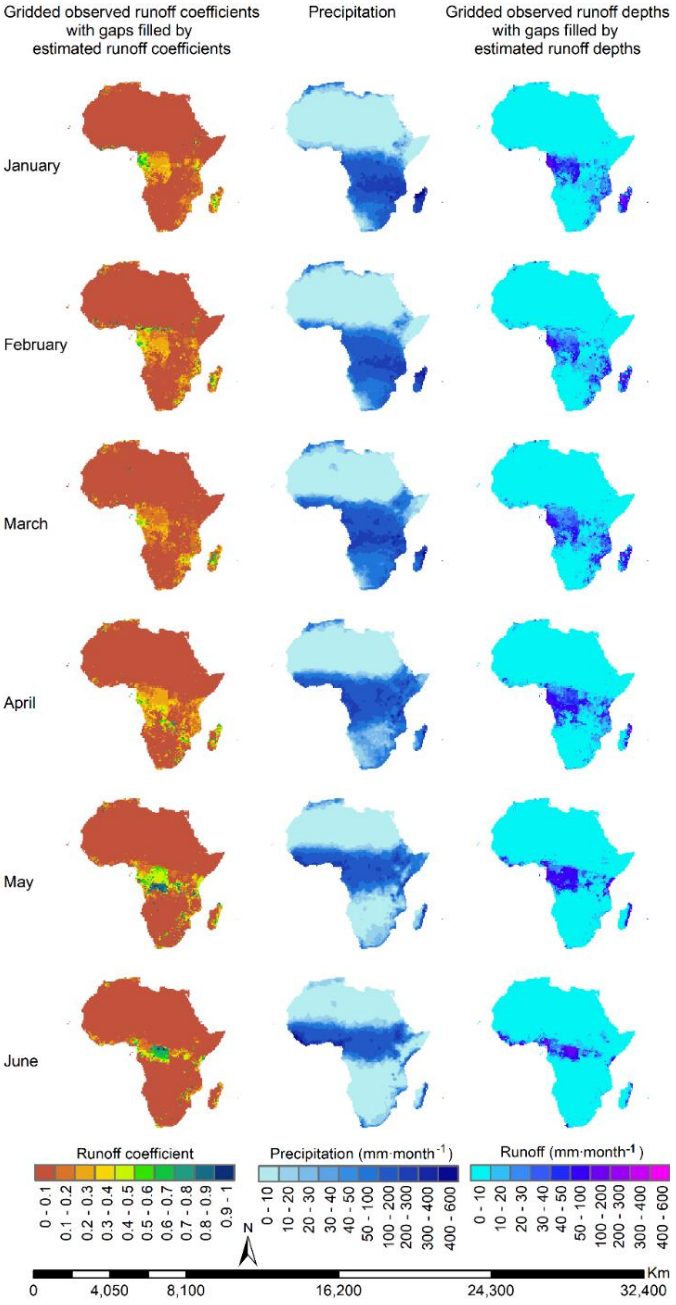

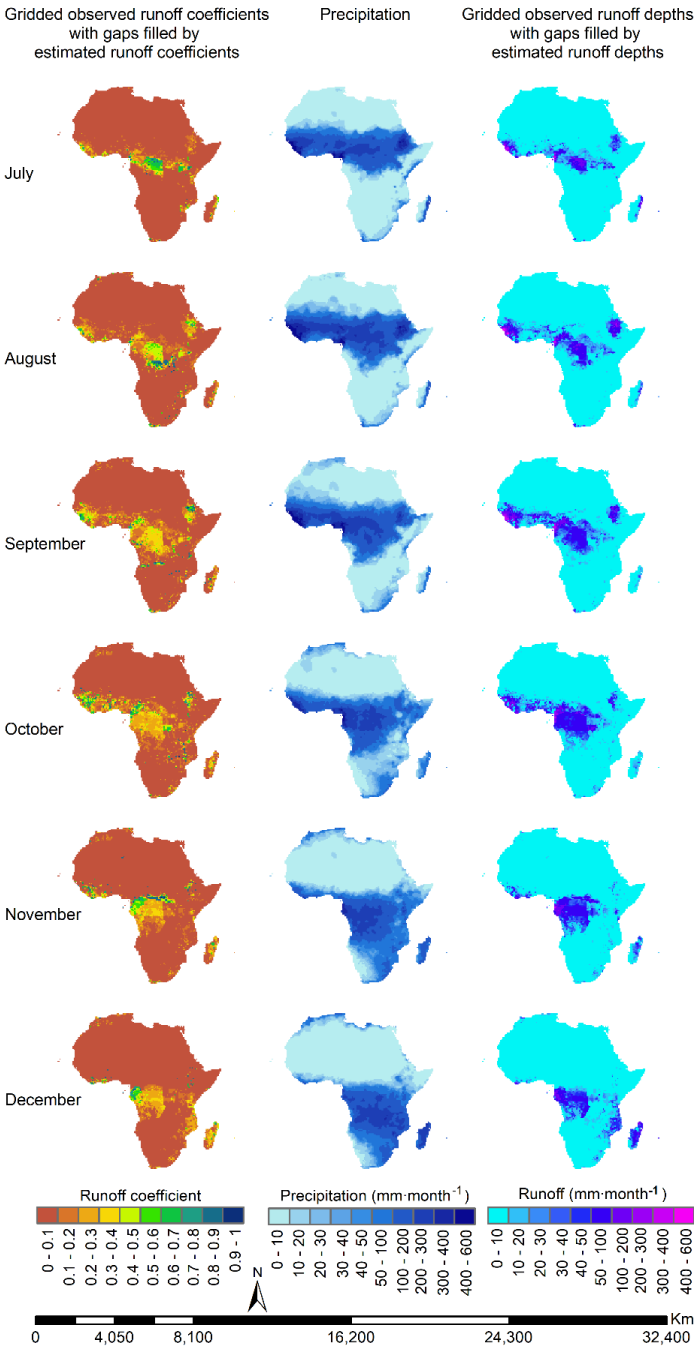
Gridded observed runoff coefficients with gaps filled by estimated runoff coefficients
Precipitation
Gridded observed runoff depths with gaps filled by estimated runoff depths
July
August
September
October
November
December
Runoff coefficient
0 - 0.1
0.1 - 0.2
0.2 - 0.3
0.3 - 0.4
0.4 - 0.5
0.5 - 0.6
0.6 - 0.7
0.7 - 0.8
0.8 - 0.9
0.9 - 1
Precipitation (mm·month-1)
0 - 10
10 - 20
20 - 30
30 - 40
40 - 50
50 - 100
100 - 200
200 - 300
300 - 400
400 - 600
Runoff (mm·month-1)
0 - 10
10 - 20
20 - 30
30 - 40
40 - 50
50 - 100
100 - 200
200 - 300
300 - 400
400 - 600
N
Km
0
4,050
8,100
16,200
24,300
32,400

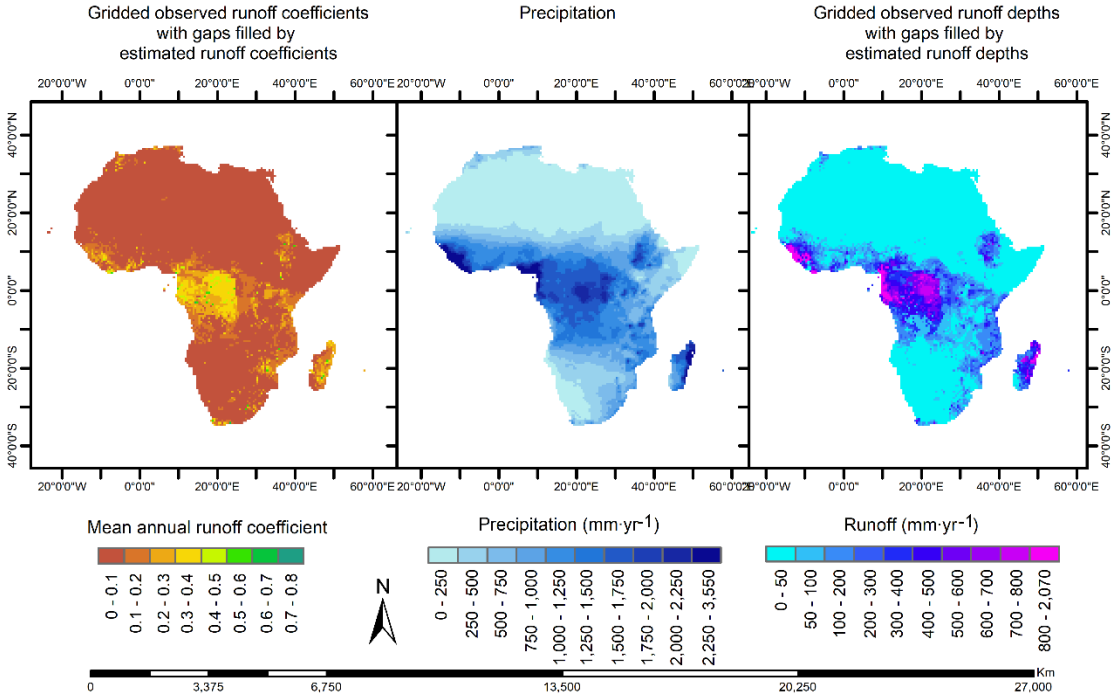


**Figure 8.** Maps of long-term mean monthly and annual runoff coefficients, precipitation and runoff depths (1901 – 2016).

### 3.1 Precipitation-runoff relationship over the continent of Africa

Zonal statistical analysis at continental level revealed that the runoff (94.9 mm·yr$^{-1}$) counts 14% of the long-term mean precipitation (671.88 mm·yr$^{-1}$) and evapotranspiration (576.98 mm·yr$^{-1}$) comprises the remaining 86% of total long-term average rainfall amount (Figure 9).

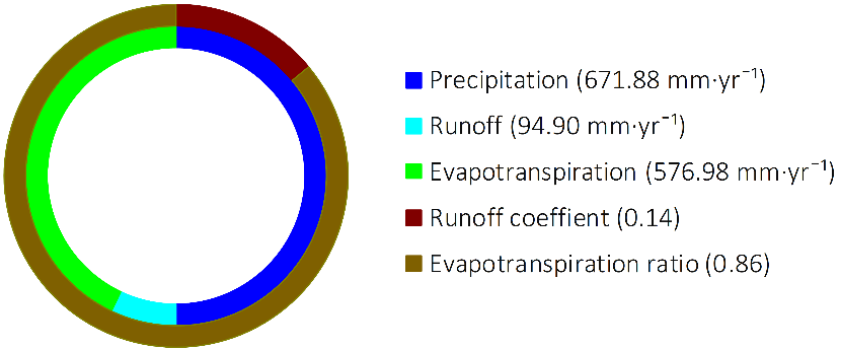


**Figure 9.** Long-term average annual water balance of Africa (1901 – 2016).

Assessment of the long-term monthly rainfall-runoff relationship revealed that the continent of Africa experienced the highest and lowest long-term mean precipitation intensities of 70.47 mm·month$^{-1}$ and 44.13 mm·month$^{-1}$ in August and June, respectively. The greatest and smallest long-term mean runoff depths of 11.20 mm·month$^{-1}$ and 5.19 mm·month$^{-1}$ are

observed in September and June, respectively. Figure 10 illustrates that the greatest rainfall-runoff correlation is recorded in October with the $R_c$ = 0.19, while the lowest $R_c$ = 0.11 is observed in July whenever P = 57.36 mm·month$^{-1}$ and R = 6.23 mm·month$^{-1}$ (Figure 10).

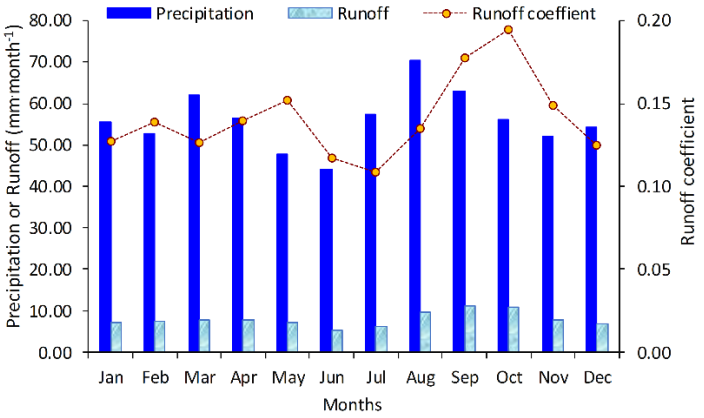


**Figure 10.** Long-term monthly precipitation-runoff relationship over the African continent (1901 – 2016).

### 3.2 Precipitation-runoff relationship within 25 major African basins

Figure 11 compares the long-term mean monthly and annual precipitation, runoff depths, runoff coefficients and long-term mean annual evapotranspiration within 25 major African basins (1901 – 2016). Top seven tropical basins out of 25 major African basins that comprised the highest runoff depths > 100 mm·yr$^{-1}$ are: Gulf of Guinea (594.35 mm·yr$^{-1}$), Madagascar (330.59 mm·yr$^{-1}$), Congo (302.28 mm·yr$^{-1}$), Africa-West Coast (278.76 mm·yr$^{-1}$), Africa-East Central Coast (159.20 mm·yr$^{-1}$), Africa-Indian Ocean Coast (147.63 mm·yr$^{-1}$), and Angola-Coast (111.32 mm·yr$^{-1}$). Apart from the Volta and Zambezi basins that also have a relatively high precipitation of 1,028.56 and 917.16 mm·yr$^{-1}$, the above-mentioned basins also comprised of highest long-term annual rainfall intensities among others, ranging from 873.71 mm·yr$^{-1}$ to 1,854.64 mm·yr$^{-1}$, and are amongst basins with the strongest correlation between rainfall and runoff compared to others with a mean runoff coefficient ranging from 0.12 to 0.32. The basins with weak precipitation-runoff relationship indicates higher $E_T$ ratios. Figure 11 also illustrates the details about monthly precipitation-runoff relationship within 25 major basins of Africa.

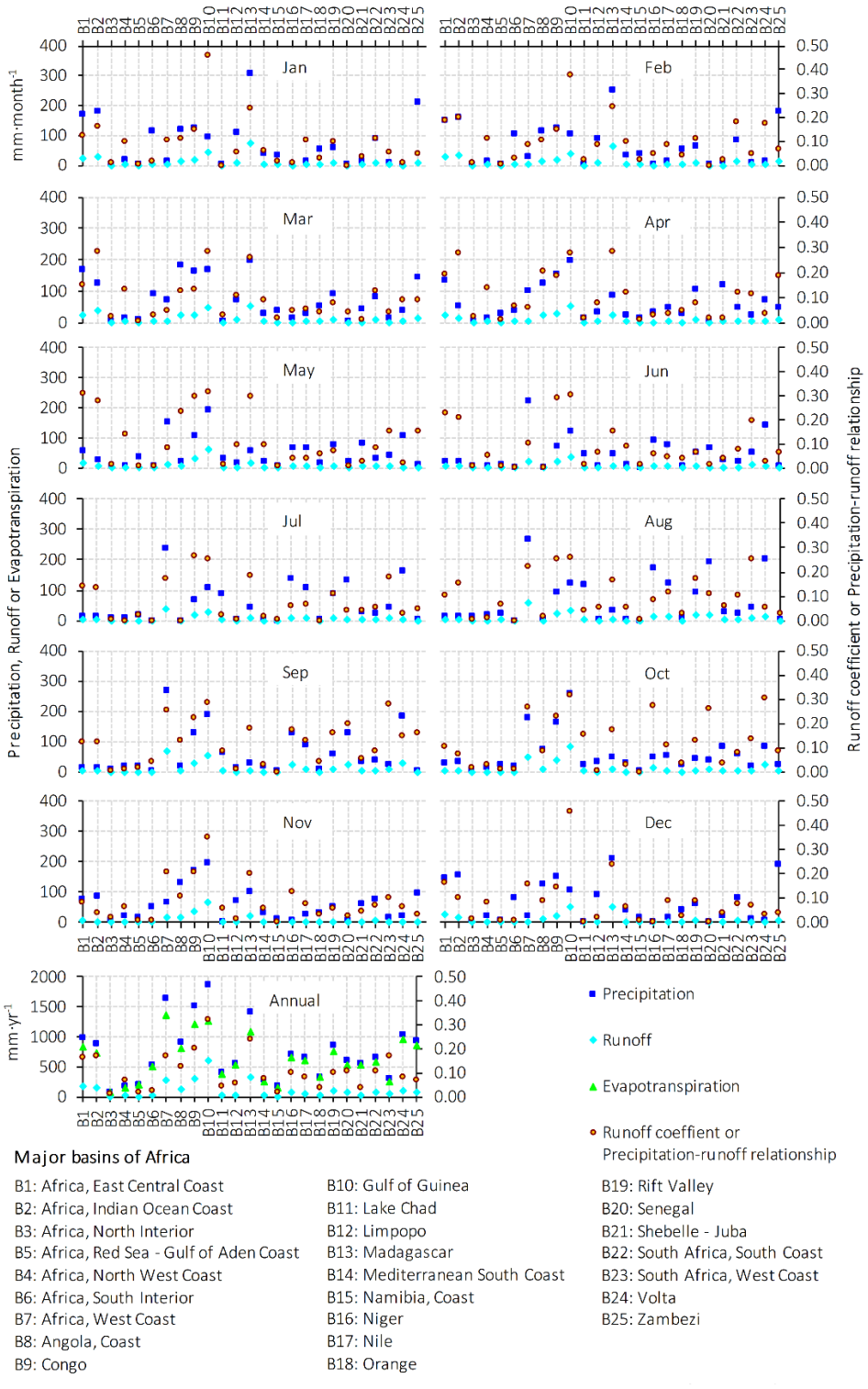


**Figure 11.** Precipitation-runoff relationship within 25 major basins of Africa (1901 – 2016).

### 3.3 Precipitation-runoff relationship within 55 African countries

Figure 12 correlates the long-term mean monthly and annual P, R and RC and long-term mean annual $E_T$ during 1901 – 2016 in 55 countries of Africa. P ranges from 16.54 mm·yr$^{-1}$ to 2,788.90 mm·yr$^{-1}$; R ranges from 0.11 mm·yr$^{-1}$ to 889.78 mm·yr$^{-1}$, in Egypt and Sierra Leone, respectively; Rc ranges from 0.004 in Western Sahara to 0.387 in Gabon. It should be noticed that, with highest runoff depths > 200 mm·yr$^{-1}$, Sierra Leone, Equatorial Guinea, Gabon, Guinea-Bissau, Republic of Congo, Cameroon, Liberia, Comoros, Seychelles, Democratic Republic of the Congo, Madagascar, São Tomé and Príncipe, Mauritius, Burundi, Guinea, and Rwanda are ranked among the top 16 out of 50 countries that experiences a relatively strongest rainfall-runoff correlation with runoff coefficients range from 0.18 to 0.32. For comparative illustration of the long-term average monthly precipitation, runoff and runoff coefficients between 55 countries of Africa, see Figure 12.

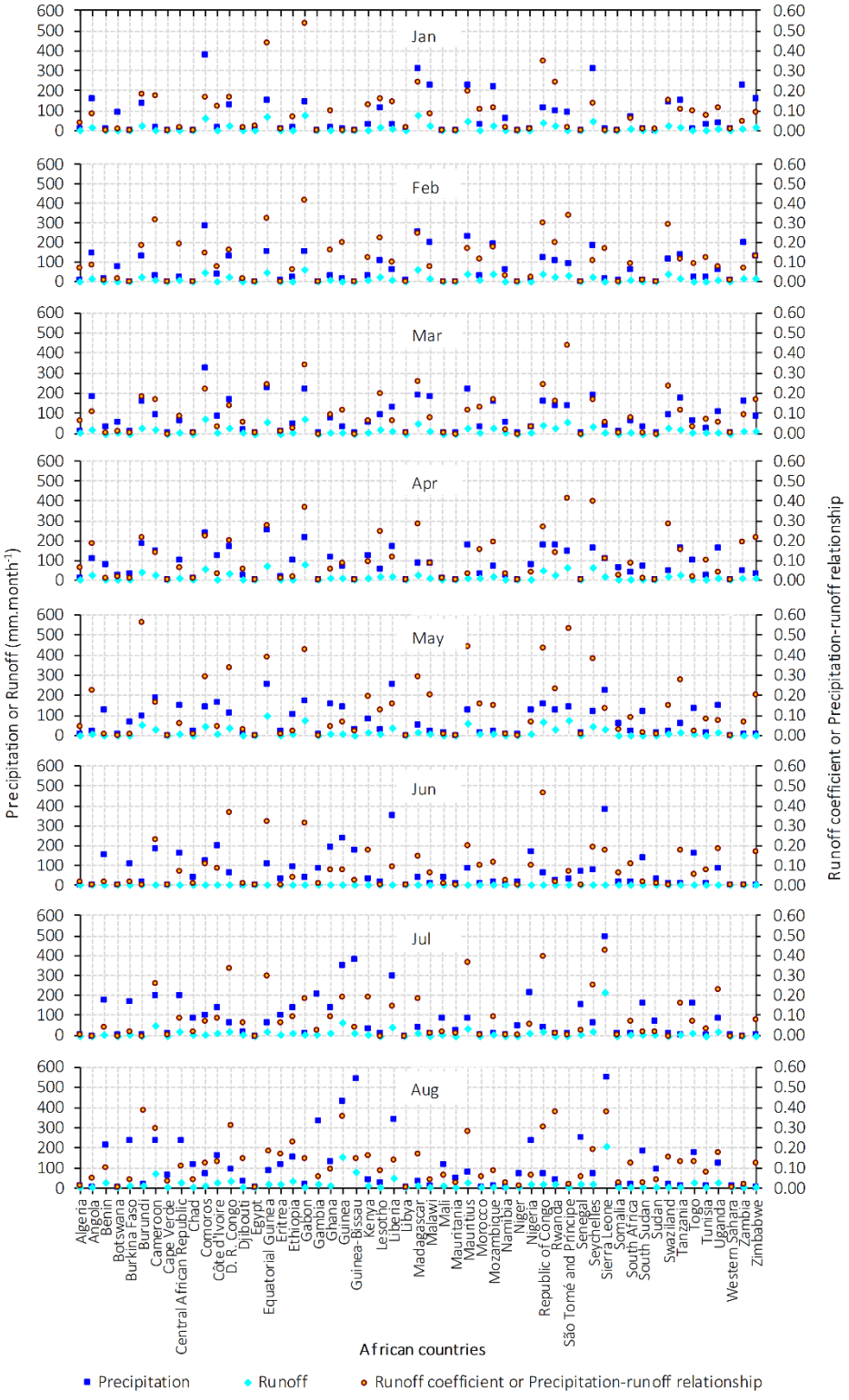
Jan
Feb
Mar
Apr
May
Jun
Jul
Aug
Precipitation or Runoff (mm.month-1)
Runoff coefficient or Precipitation-runoff relationship
African countries
Algeria
Angola
Benin
Botswana
Burkina Faso
Burundi
Cameroon
Cape Verde
Central African Republic
Chad
Comoros
Côte d'Ivoire
D. R. Congo
Djibouti
Egypt
Equatorial Guinea
Eritrea
Ethiopia
Gabon
Gambia
Ghana
Guinea
Guinea-Bissau
Kenya
Lesotho
Liberia
Libya
Madagascar
Malawi
Mali
Mauritania
Mauritius
Morocco
Mozambique
Namibia
Niger
Nigeria
Republic of Congo
Rwanda
São Tomé and Príncipe
Senegal
Seychelles
Sierra Leone
Somalia
South Africa
South Sudan
Swaziland
Tanzania
Togo
Tunisia
Uganda
Western Sahara
Zambia
Zimbabwe
Precipitation
Runoff
Runoff coefficient or Precipitation-runoff relationship

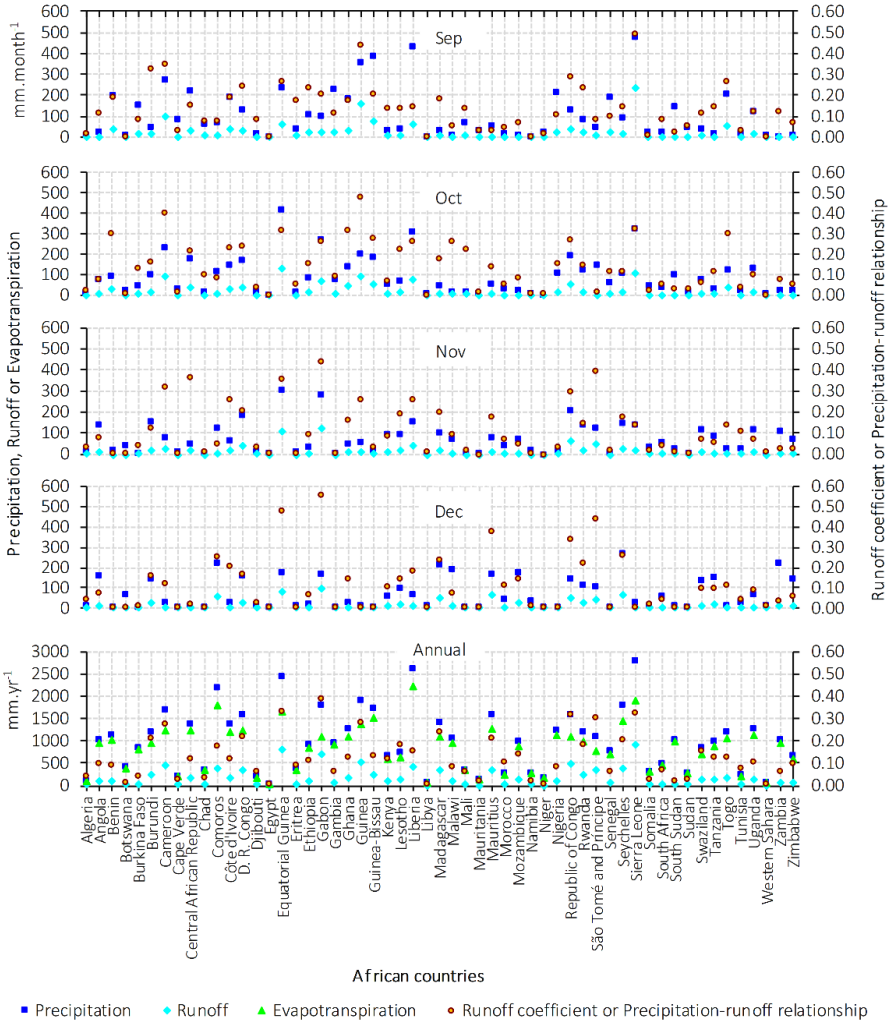


**Figure 12.** Precipitation-runoff relationship within 55 countries of Africa (1901 – 2016).

## 4 Discussions

The streamflow and rain gauging stations are known as a trustable source of reliable data for different hydrological studies (Urroz et al., 2001), but the GRDC river discharge data are available with temporal and spatial gaps mostly in low income regions including African countries (Figure 13). Obviously, trends in hydrological process are mainly associated with historical climate changes, land-cover change, reservoir storage changes, hydropower releases, and irrigation abstractions which are known to be the primary changing factors affecting the amount of rainwater flow over time (Fekete et al., 2002a). Except, the precipitation datasets available for the since the beginning of 20st century, even before, the other above-mentioned changing runoff controllers are available for the recent decades (i.e.: GRACE data for water storage change analysis were collected since 2002 and good quality land cover maps are available since 1990s). Lack of these data for the earlier decades constrained us to

predict the past runoff process. Again, if the earlier runoff discharges are excluded from the long-term runoff calculations, spatial gaps would be increased and bring more challenge for validation.

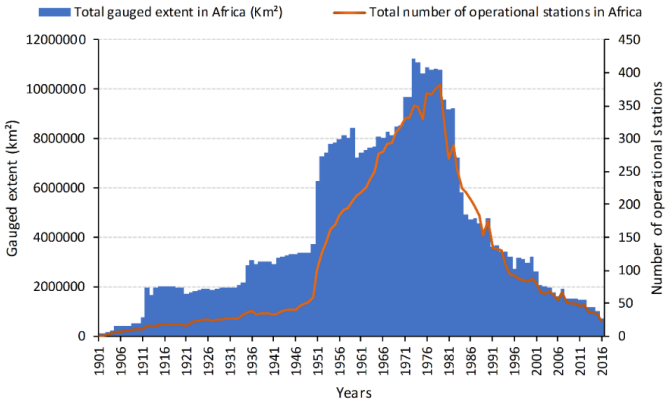


Figure 13. Historical gauged extent and number of operational stations in Africa (1901 – 2016).

A 75.64% of the total observed extent comprise the river discharges with a record of more than 20 years (Figure 3). The scarcity of runoff discharge data is common limitation in runoff prediction at a large extent such as continental scale, but they can provide reasonable results that represent the real world phenomenon (Loucks et al., 2005). Pre-analysis of the historical changes in annual runoff discharges suggested a linear trend varies between 10% and 40% among the stations which drain the catchments covered by a small extent (8.44% total gauged area). Indeed, a large proportion (91.56%) of the total African gauged area, including the catchments recorded in earlier to recent decades has stations that experienced a minor variance ranging from 0% to 10% which is not a major problem in long-term bases analysis of runoff estimation.

Actually, runoff-related studies are often conducted at a drainage basin scale, but, hydrological studies at the grid and country scales are very useful at national level since each government has own policies for water resource management. Utilization of average basin estimates directly at a country level or any other non-catchment locality seems to be unrealistic. This is the reason why this study highlighted the process of downscaling the basin' observed runoff discharges based on grids' direct runoff contributions to their corresponding basins which helps to include the effect of major runoff controlling factors (i.e.: land cover types, soil characteristics, moisture conditions and precipitation intensities) within different grids sharing the same catchment according to the Natural Resources Conservation Service (NRCS) runoff curve number (CN) method. Even though, the runoff generation process is governed by several environmental factors, but they don't have the same sensitivity and it is still too complicated to incorporate all of them in existing runoff models and methods. In this study, additional factors to those ones utilized in NRCS-CN were considered in fact that there is a considerable dissimilarity of hydrological conditions between separate catchments rather than the grids connected each other within the same catchment. It should be noticed that, the integration of NRCS-CN in downscaling the runoff discharges do not alter the quantity of observed runoff at a catchment scale, but it redistributes catchment' discharged runoff volumes to their grids according to their respective climate and physical conditions. Some runoff controlling factors such as temperature, topography, etc., are not amongst inputs of the NRCS-CN-

based direct runoff prediction, but they also have minor sensitivity a catchment or grid scale with coarse resolution. Runoff discharges were downscaled at 0.5$^{o}$ grid spatial resolution to allow their application at country analysis and facilitate their utilization on estimation over ungauged regions. Gridded observed runoff coefficients were transferred to ungauged areas using inter-gauged and ungauged parameter transfer approach. This is a Geo-spatial analysis technique acceptable for hydrological predictions in ungauged basins (PUB) (Bárdossy, 2007;Blöschl, 2006). This method assumes that two separate catchments can have a similar hydrological process when they have the same range of climatic and physical conditions. Once one of these catchments is observed it can be a source of data to unobserved one. Hydrologic similarity conditions were investigated using the runoff controlling factors selected based on their potential impact highlighted in previous studies. Thus, the efficiency analysis of the approach used to predict the data for filling the gaps suggested that the estimated and observed runoff coefficients have the goodness of fit ($R^2$) ranging from 0.56 to 0.67 for the long-term monthly Rc and 0.78 for the annual mean Rc (Figure 14). These results are within permissible validity limits since an $R^2 > 0.5$ is considered acceptable for calibration and validation in hydrological modelling (Santhi et al., 2001;Van Liew et al., 2003).

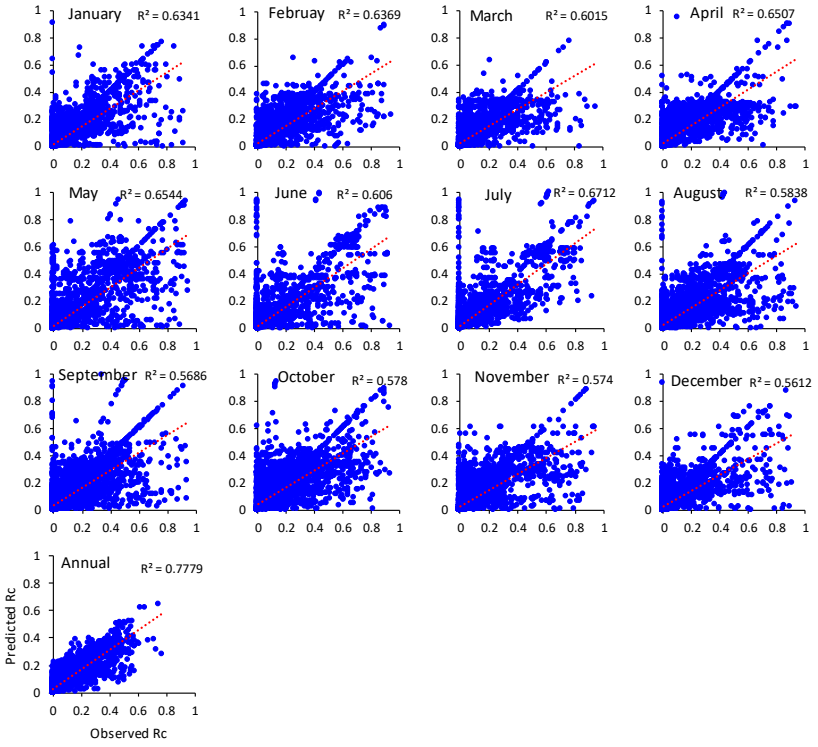


**Figure 14**. Scatter plots with a best - fit line indicating the efficiency of predicted runoff coefficients vs. gridded observed runoff coefficients over the gauged regions of Africa (Figure 7).

It can be concluded that inter-gauged and ungauged basin parameter transfer based on hydrologic similarity is an alternative approach for gaps filling in runoff prediction and it can even perform much better if the input observed runoff discharges do not have a lot of temporal gaps.

Furthermore, the study conducted by the University of New Hampshire-Global Runoff Data Centre (UNH-GRDC): "high-resolution fields of global runoff combining observed river discharge and simulated water balances" that has been considered as reference to validate the runoff-related hydrological studies since the beginning of 21st century (Fekete et al., 2002b;Hong et al., 2007) was compared with the current study based on the latitudinal zones at 1° interval scale (Figure 15). This analysis indicates that the long-term annual mean rainfall (1920 – 1980) version 2.01 (Willmott_C_J_et_al1998, 1998;Fekete et al., 2002b) that was utilized to simulate the UNH/GRDC composite runoff (Fekete et al., 2002b) is roughly matching with the long-term (1901 – 2016) mean annual GPCC precipitation estimated in the current study (Figure 15). Our comparative analysis also shows better agreements over the northern hemisphere between 36°N and 14°N, in the southern hemisphere between 17°S and 34°S latitudes, and in the equatorial zone laying between 4°N and 8°S. Major differences are between 14°N and 4°N in the northern hemisphere and in the southern hemisphere between 8°S and 17°S latitudes. These differences are possibly due to the UNH/GRDC method that assigned the same runoff depths in observed and unobserved basins that led to overestimation of the runoff in drylands of Australia and Africa and gridded runoff depth that was estimated by considering rainfall factor alone (Fekete et al., 2002). The latitudinal profile analysis revealed that on the 2°S latitude is the runoff hotspot region of Africa with higher mean R depth (387.65 mm·yr$^{-1}$) and P (1,422.77 mm·yr$^{-1}$), and a relatively strongest P-R correlation with Rc of 0.27, followed by the 1°S latitude zone with the R of 383.87 mm·yr$^{-1}$, P of 1,504.47 mm·yr$^{-1}$, and Rc of 0.26, and as well equatorial zone at 0° latitude with a mean R of 379.99 mm·yr$^{-1}$, P of 1,490.18 mm·yr$^{-1}$, and Rc of 0.25.

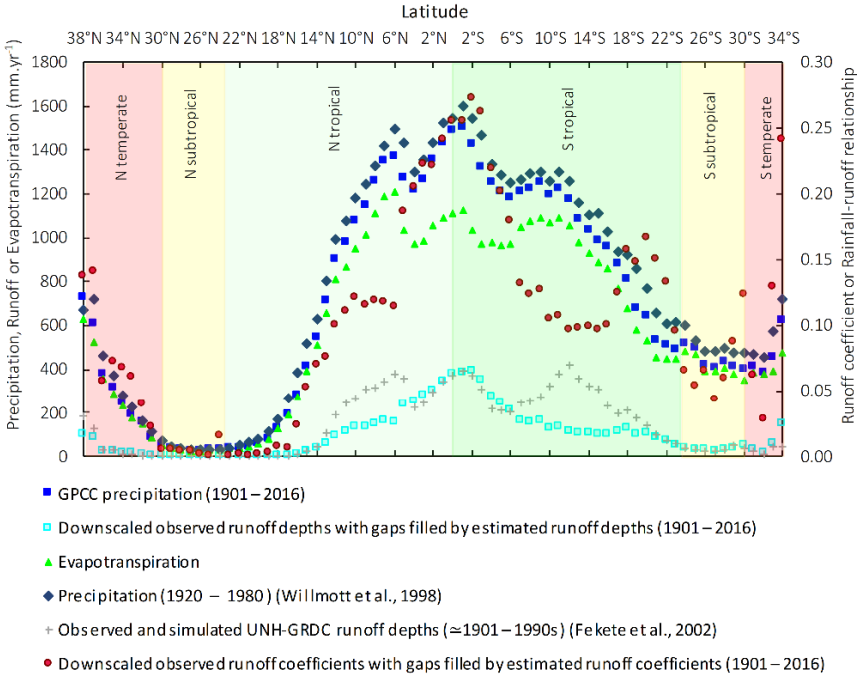


**Figure 15.** Comparison of the precipitation-runoff relationship between the UNH-GRDC (Fekete et al., 2002b) and the present study.

Based on the following six latitudinal climate zones northern (N) tropical (0°Equator ≤ latitude ≤ 23.4°N), southern (S) tropical (23.4°S ≤ latitude < 0°Equator), N subtropics (23.4°N ≤ latitude ≤ 30°N), S subtropics (23.4°S ≤ latitude ≤ 30°S), N temperate

(30°N < latitude ≤ 72°N), and S temperate (30°S < latitude ≤ 72°S) (Peel et al., 2007), the long-term annual mean of the water balance's variables, including precipitation (P), evapotranspiration ($E_T$), runoff (R) and their corresponding runoff coefficients (Rc) for the period of 116 years (1901 – 2016) were estimated and presented in Table 4 to provide tangible statistics corresponding to Figure 15.

**Table 4.** Long-term annual water balance and runoff coefficients within the African latitudinal climatic zones (1901 – 2016).

| Latitudinal climatic zones | % area Africa | P (mm·yr$^{-1}$) | $E_T$ (mm·yr$^{-1}$) | R (mm·yr$^{-1}$) | Rc |
|---|---|---|---|---|---|
| **Tropical** | **75** | **836.36** | **713.70** | **122.66** | **0.15** |
| N tropical | 48 | 708.94 | 615.72 | 93.22 | 0.13 |
| S tropical | 26 | 1,070.13 | 893.45 | 176.68 | 0.17 |
| **Subtropics** | **17** | **146.23** | **138.03** | **8.20** | **0.06** |
| N subtropical | 13 | 28.35 | 28.22 | 0.13 | 0.00 |
| S subtropical | 5 | 455.27 | 425.91 | 29.36 | 0.06 |
| **Temperate zones** | **8** | **257.34** | **236.94** | **20.40** | **0.08** |
| N temperate | 6 | 207.51 | 193.79 | 13.72 | 0.07 |
| S temperate | 2 | 423.94 | 381.21 | 42.73 | 0.10 |

Compared to the tropical zone, subtropical and temperate zones of Africa have low rainfall and runoff amounts (Figure 15 and Table 4), which may expose them to the water scarcity (Maliva and Missimer, 2012). The countries and basins located in the tropical zone are often prone to a higher precipitation intensity which produce huge runoff volumes enough for underground and surface water replenishment, however, some time causing stormwater-related disasters (Ponette-González et al., 2015;Karamage et al., 2017b).

## 5 Conclusions

This study has highlighted step by step how the Natural Resources Conservation Service (NRCS) runoff curve number (CN) can be a prominent proxy for the basin's river discharge downscaling at a grid scale which can be reasonably utilized on non-catchment regional studies. This approach helped us to produce gridded long-term monthly runoff depths and coefficients datasets used to analyze the spatial relationship between precipitation and runoff over all 55 countries and 25 major drainage basins covering the whole continent of Africa. The Global Runoff Data Centre (GRDC)'s streamflow records available for 535 catchments covering ≃ 47.43% of the total African continent became a source of information for predicting the P-R correlation over ungauged regions based on the inter-gauged and ungauged parameter transfer approach and spatial hydrologic similarity analysis assed using the key runoff controlling factors including antecedent moisture condition (AMC), NRCS-CN, terrestrial water storage, temperature, topographic wetness index (TWI), and slope. Both higher runoff depths and strong P-R correlation were observed in the tropical humid regions due to their intensive precipitation more than in subtropical and

temperate zones. This study suggests the need for rehabilitation awareness of operational stream gauging stations and establishment of new ones where they are necessary to make sure streamflow are regularly and widely recorded in different catchments of Africa to provide sufficient update data required for accurate water resource planning.

**Acknowledgments:** Many thanks to the editor and anonymous referees for the insightful comments that helped us to improve the quality of this manuscript. This study was supported by: (a) the Chinese Academy of Sciences and the World Academy of Sciences (CAS-TWAS) President's PhD Fellowship Program, and (b) the Sino-Africa Joint Research Centre, Chinese Academy of Sciences (No. SAJC201609).

## References

Abdi, A. M., Boke-Olén, N., Tenenbaum, D. E., Tagesson, T., Cappelaere, B., and Ardö, J.: Evaluating water controls on vegetation growth in the semi-arid Sahel using field and Earth observation data, Remote Sensing, 9, 294, 2017.

Anja, M.-C., Andreas, B., Peter, F., Udo, S., and Markus, Z.: GPCC Climatology Version 2018 at 0.5°: Monthly Land-Surface Precipitation Climatology for Every Month and the Total Year from Rain-Gauges built on GTS-based and Historical Data. DOI: 10.5676/DWD_GPCC/CLIM_M_V2018_050, 2018.

Bárdossy, A.: Calibration of hydrological model parameters for ungauged catchments, Hydrology and Earth System Sciences Discussions, 11, 703-710, 2007.

Beck, H. E., de Jeu, R. A., Schellekens, J., van Dijk, A. I., and Bruijnzeel, L. A.: Improving curve number based storm runoff estimates using soil moisture proxies, IEEE Journal of selected topics in applied earth observations and remote sensing, 2, 250-259, 2009.

BEVEN, K. J., and Kirkby, M. J.: A physically based, variable contributing area model of basin hydrology/Un modèle à base physique de zone d'appel variable de l'hydrologie du bassin versant, Hydrological Sciences Journal, 24, 43-69, 1979.

Blöschl, G.: Rainfall-runoff modeling of ungauged catchments, Encyclopedia of hydrological sciences, 2006.

Blume, T., Zehe, E., and Bronstert, A.: Rainfall—runoff response, event-based runoff coefficients and hydrograph separation, Hydrological Sciences Journal, 52, 843-862, 2007.

Brown, J. L., Bennett, J. R., and French, C. M.: SDMtoolbox 2.0: the next generation Python-based GIS toolkit for landscape genetic, biogeographic and species distribution model analyses, PeerJ, 5, e4095, 2017.

Cervigni, R., and Morris, M.: Confronting Drought in Africa's Drylands: Opportunities for Enhancing Resilience, World Bank Publications, 2016.

Chen, L., Liu, C., Li, Y., and Wang, G.: Impacts of climatic factors on runoff coefficients in source regions of the Huanghe River, Chinese Geographical Science, 17, 047-055, 2007.

Chiew, F., Zheng, H., and Potter, N.: Rainfall-Runoff Modelling Considerations to Predict Streamflow Characteristics in Ungauged Catchments and under Climate Change, Water, 10, 1319, 2018.

Clover, J.: Food security in sub-saharan Africa: feature, African security review, 12, 5-15, 2003.

Cook, K. H., and Vizy, E. K.: Detection and analysis of an amplified warming of the Sahara Desert, Journal of Climate, 28, 6560-6580, 2015.

Cosgrove, W. J., and Loucks, D. P.: Water management: Current and future challenges and research directions, Water Resources Research, 51, 4823-4839, 10.1002/2014wr016869, 2015.

Cronshey, R.: Urban hydrology for small watersheds, US Dept. of Agriculture, Soil Conservation Service, Engineering Division, 1986.

Dewitte, O., Jones, A., Spaargaren, O., Breuning-Madsen, H., Brossard, M., Dampha, A., Deckers, J., Gallali, T., Hallett, S., and Jones, R.: Harmonisation of the soil map of Africa at the continental scale, Geoderma, 211, 138-153, 2013.

Edwards, P. J., Williard, K. W., and Schoonover, J. E.: Fundamentals of watershed hydrology, Journal of Contemporary Water Research & Education, 154, 3-20, 2015.

Engineers, U. A. C.: Hydrologic modeling system (HEC-HMS) application guide: version 3.1. 0, Institute for Water Resources, Davis, 2008.

Land Cover CCI PRODUCT USER GUIDE VERSION 2.0, DOCUMENT REF: CCI-LC-PUGV2: http://maps.elie.ucl.ac.be/CCI/viewer/download/ESACCI-LC-Ph2-PUGv2_2.0.pdf, access: 15 January, 2017.

Hydrological basins in Africa (Derived from HydroSHEDS). http://www.fao.org/geonetwork/srv/en/main.search?any=awrd&themekey=%22watersheds%22, 2009.

Fekete, B. M., Vörösmarty, C. J., and Grabs, W.: High-resolution fields of global runoff combining observed river discharge and simulated water balances, Global Biogeochemical Cycles, 16, 15-11-15-10, 2002a.
Fekete, B. M., Vörösmarty, C. J., and Grabs, W.: High-resolution fields of global runoff combining observed river discharge and simulated water balances, Global Biogeochemical Cycles, 16, 2002b.
Fernandez-Illescas, C. P., Porporato, A., Laio, F., and Rodriguez-Iturbe, I.: The ecohydrological role of soil texture in a water-limited ecosystem, Water Resources Research, 37, 2863-2872, 2001.
GADM: Global Administrative Areas (GADM), version 2.8, November 2015. www.gadm.org, 2015.
Goudie, A.: The human impact on the natural environment, MIT press, 2000.
The Global Runoff Data Centre, 56068 Koblenz, Germany. http://www.bafg.de/GRDC/EN/02_srvcs/21_tmsrs/riverdischarge_node.html, 2018.
Halwatura, D., and Najim, M.: Application of the HEC-HMS model for runoff simulation in a tropical catchment, Environmental modelling & software, 46, 155-162, 2013.
Harris, I., Jones, P., Osborn, T., and Lister, D.: Updated high-resolution grids of monthly climatic observations–the CRU TS3. 10 Dataset, International Journal of Climatology, 34, 623-642, 2014.
Hawkins, R. H.: Asymptotic determination of runoff curve numbers from data, Journal of Irrigation and Drainage Engineering, 119, 334-345, 1993.
Heggen, R. J.: Normalized antecedent precipitation index, Journal of hydrologic Engineering, 6, 377-381, 2001.
Hengl, T., de Jesus, J. M., MacMillan, R. A., Batjes, N. H., Heuvelink, G. B., Ribeiro, E., Samuel-Rosa, A., Kempen, B., Leenaars, J. G., and Walsh, M. G.: SoilGrids1km—global soil information based on automated mapping, PLoS One, 9, e105992, 2014.
Hengl, T., Heuvelink, G. B., Kempen, B., Leenaars, J. G., Walsh, M. G., Shepherd, K. D., Sila, A., MacMillan, R. A., de Jesus, J. M., and Tamene, L.: Mapping soil properties of Africa at 250 m resolution: random forests significantly improve current predictions, PloS one, 10, e0125814, 2015.
Hong, Y., Adler, R. F., Hossain, F., Curtis, S., and Huffman, G. J.: A first approach to global runoff simulation using satellite rainfall estimation, Water Resources Research, 43, 2007.
Jaleta, D., Mbilinyi, B. P., Mahoo, H. F., and Lemenih, M.: Effect of Eucalyptus expansion on surface runoff in the central highlands of Ethiopia, Ecological Processes, 6, 1, 2017.
Kadioglu, M., and ŞEN, Z.: Monthly precipitation-runoff polygons and mean runoff coefficients, Hydrological Sciences Journal, 46, 3-11, 2001.
Karamage, F., Zhang, C., Ndayisaba, F., Nahayo, L., Kayiranga, A., Omifolaji, J. K., Shao, H., Umuhoza, A., Nsengiyumva, J. B., and Liu, T.: The need for awareness of drinking water loss reduction for sustainable water resource management in Rwanda, Journal of Geoscience and Environment Protection, 4, 74, 2016.
Karamage, F., Zhang, C., Fang, X., Liu, T., Ndayisaba, F., Nahayo, L., Kayiranga, A., and Nsengiyumva, J. B.: Modeling rainfall-runoff response to land use and land cover change in Rwanda (1990–2016), Water, 9, 147, 2017a.
Karamage, F., Zhang, C., Liu, T., Maganda, A., and Isabwe, A.: Soil Erosion Risk Assessment in Uganda, Forests, 8, 52, 2017b.
Knisel, W., and Douglas-Mankin, K.: CREAMS/GLEAMS: Model use, calibration, and validation, Transactions of the ASABE, 55, 1291-1302, 2012.
Kohler, M. A., and Linsley, R. K.: Predicting the runoff from storm rainfall, US Department of Commerce, Weather Bureau Washington, DC, 1951.
Lehner, B., Verdin, K., and Jarvis, A.: New global hydrography derived from spaceborne elevation data, Eos, Transactions American Geophysical Union, 89, 93-94, 2008.
Lim, K. J., Engel, B. A., Muthukrishnan, S., and Harbor, J.: EFFECTS OF INITIAL ABSTRACTION AND URBANIZATION ON ESTIMATED RUNOFF USING CN TECHNOLOGY 1, JAWRA Journal of the American Water Resources Association, 42, 629-643, 2006.
Liu, T., Yan, H., and Zhai, L.: Extract relevant features from DEM for groundwater potential mapping, The International Archives of Photogrammetry, Remote Sensing and Spatial Information Sciences, 40, 113, 2015.
Liu, Y., and De Smedt, F.: WetSpa extension, a GIS-based hydrologic model for flood prediction and watershed management, Vrije Universiteit Brussel, Belgium, 1-108, 2004.
Long, D., Longuevergne, L., and Scanlon, B. R.: Uncertainty in evapotranspiration from land surface modeling, remote sensing, and GRACE satellites, Water Resources Research, 50, 1131-1151, 2014.
Loucks, D., Van Beek, E., Stedinger, J., Dijkman, J., and Villars, M.: Model sensitivity and uncertainty analysis, Water resources systems planning and management, 255-290, 2005.
Mahmoud, S. H.: Investigation of rainfall–runoff modeling for Egypt by using remote sensing and GIS integration, Catena, 120, 111-121, 2014.
Maliva, R., and Missimer, T.: Arid lands water evaluation and management, Springer Science & Business Media, 2012.
Markus, Z., Armin, R.-S., Andreas, B., Peter, F., Anja, M.-C., and Udo, S.: GPCC Full Data Daily Version.2018 at 1.0°: Daily Land-Surface Precipitation from Rain-Gauges built on GTS-based and Historic Data. DOI: 10.5676/DWD_GPCC/FD_D_V2018_100, 2018.

Mawere, M.: Underdevelopment, Development and the Future of Africa, Langaa Rpcig, 2017.
McCabe, G. J., and Wolock, D. M.: Independent effects of temperature and precipitation on modeled runoff in the conterminous United States, Water Resources Research, 47, 2011.
Messer, E., Cohen, M. J., and Marchione, T.: Conflict: A cause and effect of hunger, Environmental Change and Security Project Report, 7, 1-16, 2001.
Mishra, S., Sahu, R., Eldho, T., and Jain, M.: An improved I a S relation incorporating antecedent moisture in SCS-CN methodology, Water Resources Management, 20, 643-660, 2006.
Mishra, S. K., and Singh, V. P.: A relook at NEH-4 curve number data and antecedent moisture condition criteria, Hydrological Processes: An International Journal, 20, 2755-2768, 2006.
Moucha, R., and Forte, A. M.: Changes in African topography driven by mantle convection, Nature Geoscience, 4, 707, 2011.
Murray-Tortarolo, G., Jaramillo, V. J., Maass, M., Friedlingstein, P., and Sitch, S.: The decreasing range between dry-and wet-season precipitation over land and its effect on vegetation primary productivity, PloS one, 12, e0190304, 2017.
Ogden, F. L., Raj Pradhan, N., Downer, C. W., and Zahner, J. A.: Relative importance of impervious area, drainage density, width function, and subsurface storm drainage on flood runoff from an urbanized catchment, Water Resources Research, 47, 2011.
Olang, L., and Fürst, J.: Effects of land cover change on flood peak discharges and runoff volumes: model estimates for the Nyando River Basin, Kenya, Hydrological Processes, 25, 80-89, 2011.
Oyebande, L.: Water problems in Africa—how can the sciences help?, Hydrological Sciences Journal, 46, 947-962, 2001.
Paul, J. D., Roberts, G. G., and White, N.: The African landscape through space and time, Tectonics, 33, 898-935, 2014.
Peel, M. C., Finlayson, B. L., and McMahon, T. A.: Updated world map of the Köppen-Geiger climate classification, Hydrology and earth system sciences discussions, 4, 439-473, 2007.
Penman, J., Gytarsky, M., Hiraishi, T., Krug, T., Kruger, D., Pipatti, R., Buendia, L., Miwa, K., Ngara, T., and Tanabe, K.: Good practice guidance for land use, land-use change and forestry, Good practice guidance for land use, land-use change and forestry., 2003.
Ponce, V. M., and Hawkins, R. H.: Runoff curve number: Has it reached maturity?, Journal of hydrologic engineering, 1, 11-19, 1996.
Ponette-González, A. G., Brauman, K. A., Marín-Spiotta, E., Farley, K. A., Weathers, K. C., Young, K. R., and Curran, L. M.: Managing water services in tropical regions: From land cover proxies to hydrologic fluxes, Ambio, 44, 367-375, 2015.
Ruess, P.: Mapping of Water Stress Indicators, 2015.
Santhi, C., Arnold, J. G., Williams, J. R., Dugas, W. A., Srinivasan, R., and Hauck, L. M.: Validation of the swat model on a large rwer basin with point and nonpoint sources 1, JAWRA Journal of the American Water Resources Association, 37, 1169-1188, 2001.
Save, H., Bettadpur, S., and Tapley, B. D.: High-resolution CSR GRACE RL05 mascons, Journal of Geophysical Research: Solid Earth, 121, 7547-7569, 2016.
Sayre, and Pulley, A.: Africa, Twenty-First Century Books, 1999.
Schuol, J., Abbaspour, K. C., Yang, H., Srinivasan, R., and Zehnder, A. J.: Modeling blue and green water availability in Africa, Water Resources Research, 44, 2008.
Shi, Z.-H., Chen, L.-D., Fang, N.-F., Qin, D.-F., and Cai, C.-F.: Research on the SCS-CN initial abstraction ratio using rainfall-runoff event analysis in the Three Gorges Area, China, Catena, 77, 1-7, 2009.
Silveira, L., Charbonnier, F., and Genta, J.: The antecedent soil moisture condition of the curve number procedure, Hydrological Sciences Journal, 45, 3-12, 2000.
Smakhtin, V.: Taking into account environmental water requirements in global-scale water resources assessments, Iwmi, 2004.
Sörensen, R., Zinko, U., and Seibert, J.: On the calculation of the topographic wetness index: evaluation of different methods based on field observations, Hydrology and Earth System Sciences Discussions, 10, 101-112, 2006.
Sumarauw, J. S. F., and Ohgushi, K.: Analysis on curve number, land use and land cover changes and the impact to the peak flow in the Jobaru River Basin, Japan, International Journal of Civil & Environmental Engineering IJCEE-IJENS, 12, 17-23, 2012.
Terakawa, A.: Hydrological data management: Present state and trends, Secretariat of the World Meteorological Organization, 2003.
Tesemma, Z. K., Mohamed, Y. A., and Steenhuis, T. S.: Trends in rainfall and runoff in the Blue Nile Basin: 1964–2003, Hydrological processes, 24, 3747-3758, 2010.
United Nations, Department of Economic and Social Affairs, Population Division (2017). World Population Prospects: The 2017 Revision, Key Findings and Advance Tables. ESA/P/WP/248. https://esa.un.org/unpd/wpp/Publications/, 2017.
UNISDR: Global Assessment Report on Disaster Risk Reduction (GAR 2011). https://www.preventionweb.net/english/hyogo/gar/, 2011.
UNISDR: Global Assessment Report on Disaster Risk Reduction (GAR 2015). https://www.preventionweb.net/english/hyogo/gar/, 2015.
Urroz, G., Leines, R. C., Perret, G. L., Holland, J. M., and Hunsaker, B. E.: Development of a Low-cost, Self-calibrating Stream Gaging Station, 2001.
Van Liew, M., Arnold, J., and Garbrecht, J.: Hydrologic simulation on agricultural watersheds: Choosing between two models, Transactions of the ASAE, 46, 1539, 2003.
Viessman Jr, W., and Knapp, J. W.: Introduction to hydrology, 1977.
Walkenbach, J.: Excel 2010 power programming with VBA, John Wiley & Sons, 2010.

Weng, Q.: Modeling urban growth effects on surface runoff with the integration of remote sensing and GIS, Environmental management, 28, 737-748, 2001.
Global Air Temperature and Precipitation Climatologies, by : Cort J. Willmott, Kenji Matsuura and David R. Legates (Center for Climate Research, University of Deleware), version 2.01, November 1998: https://rda.ucar.edu/datasets/ds236.0/, access: 15 January, 1998.
Woodward, D. E., Hawkins, R. H., Jiang, R., Hjelmfelt, J., Allen T, Van Mullem, J. A., and Quan, Q. D.: Runoff curve number method: examination of the initial abstraction ratio, World water & environmental resources congress 2003, 2003, 1-10,
Wright, J. R., and Skiles, J.: SPUR Simulation of Production and Utilization of Rangelands: Documentation and User Guide, USDA-Agricultural Research Service, Northwest Watershed Research Center, 1987.
Xiao, Y., Yi, S., and Tang, Z.: Integrated flood hazard assessment based on spatial ordered weighted averaging method considering spatial heterogeneity of risk preference, Science of the Total Environment, 599, 1034-1046, 2017.
Yeo, I.-Y., Gordon, S. I., and Guldmann, J.-M.: Optimizing patterns of land use to reduce peak runoff flow and nonpoint source pollution with an integrated hydrological and land-use model, Earth Interactions, 8, 1-20, 2004.
Yuan, Y., Nie, W., McCutcheon, S. C., and Taguas, E. V.: Initial abstraction and curve numbers for semiarid watersheds in Southeastern Arizona, Hydrological Processes, 28, 774-783, 2014.
Yuting, F., Yaning, C., Weihong, L., HuaiJun, W., and XinGong, L.: Impacts of temperature and precipitation on runoff in the Tarim River during the past 50 years, 干旱区科学, 3, 220-230, 2011.
Zeng, Z., Tang, G., Hong, Y., Zeng, C., and Yang, Y.: Development of an NRCS curve number global dataset using the latest geospatial remote sensing data for worldwide hydrologic applications, Remote Sensing Letters, 8, 528-536, 2017.
Zhu, X.: GIS for Environmental Applications: A practical approach, Routledge, 2016.


**Figure 16: The logo of Copernicus Publications.**